



Measurement of CKM matrix elements in single top quark t -channel production in proton-proton collisions at $\sqrt{s} = 13$ TeV

The CMS Collaboration*

Abstract

The first direct, model-independent measurement is presented of the modulus of the Cabibbo–Kobayashi–Maskawa (CKM) matrix elements $|V_{tb}|$, $|V_{td}|$, and $|V_{ts}|$, in final states enriched in single top quark t -channel events. The analysis uses proton-proton collision data from the LHC, collected during 2016 by the CMS experiment, at a centre-of-mass energy of 13 TeV, corresponding to an integrated luminosity of 35.9 fb^{-1} . Processes directly sensitive to these matrix elements are considered at both the production and decay vertices of the top quark. In the standard model hypothesis of CKM unitarity, a lower limit of $|V_{tb}| > 0.970$ is measured at the 95% confidence level. Several theories beyond the standard model are considered, and by releasing all constraints among the involved parameters, the values $|V_{tb}| = 0.988 \pm 0.024$, and $|V_{td}|^2 + |V_{ts}|^2 = 0.06 \pm 0.06$, where the uncertainties include both statistical and systematic components, are measured.

"Published in Physics Letters B as doi:10.1016/j.physletb.2020.135609."

1 Introduction

A distinctive feature of the electroweak sector of top quark physics is the relative magnitude of the Cabibbo–Kobayashi–Maskawa (CKM) [1] matrix element V_{tb} with respect to V_{td} and V_{ts} , which leads to a strong suppression of processes involving mixing between the third and the first two quark families. This feature can be probed at the CERN LHC by studying the couplings of top quarks to d, s, and b quarks in electroweak charged-current interactions, where such couplings play a role at either the production or decay vertices of the top quark. In general, top quarks are produced in proton-proton (pp) collisions through the strong interaction, predominantly via gluon fusion, creating a top quark-antiquark ($t\bar{t}$) pair. Top quarks can also be singly produced via the electroweak interaction, in which case the dominant mechanism involves an exchange of a W boson in the t channel, a process which has been precisely measured at the LHC [2–11]. The dominant decay process for a top quark is to a W boson and a b quark via an electroweak charged-current interaction. All single top quark processes therefore allow the direct probing of the tWq vertex, with q representing a b, d, or s quark, both in production and decay of the top quark. In the t channel, a top quark is produced recoiling against a light quark, henceforth referred to as q' . Figure 1 shows typical Feynman diagrams at leading order (LO) for the different production and decay modes considered in this analysis.

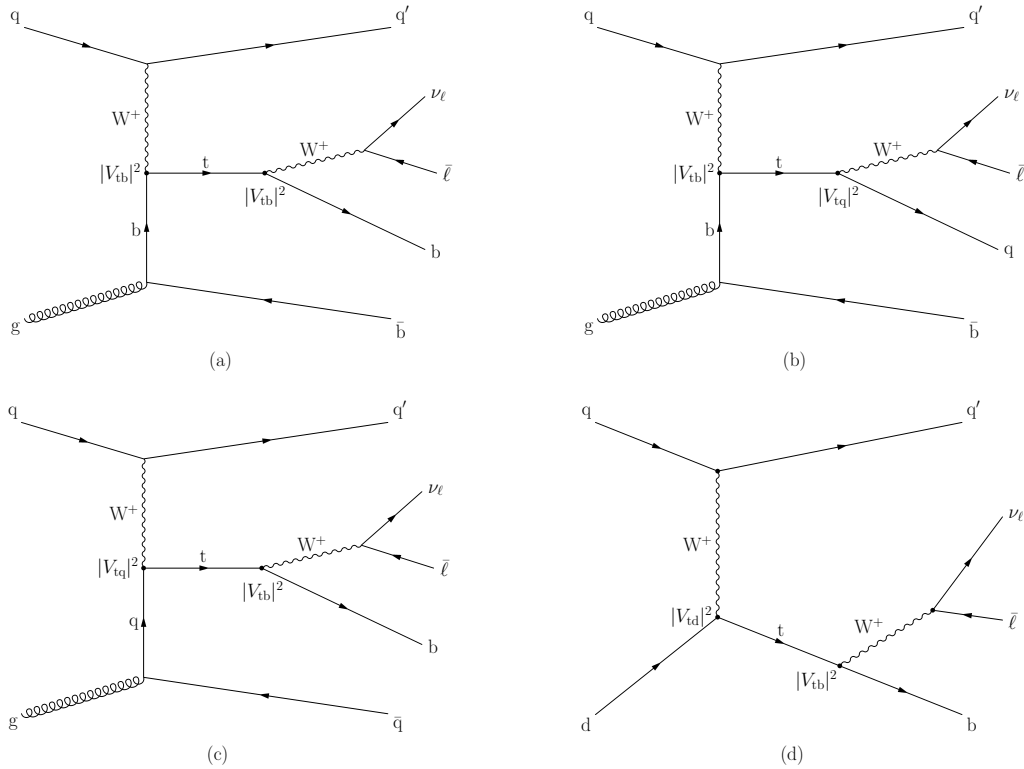


Figure 1: Leading-order Feynman diagrams for single top quark production via the t channel featuring: (a) a tWb vertex in production and decay, (b) a tWb vertex in production and a tWq in decay, with q being an s or d quark, (c) a tWq vertex in production and a tWb in decay, and (d) a process initiated by a d quark and enhanced due to contributions from these valence quarks. The ℓ refers to e or μ leptons.

The elements V_{tb} , V_{td} , and V_{ts} of the CKM matrix can be indirectly constrained from measurements in the B and K meson sectors [12], but those determinations rely crucially on model assumptions, such as the existence of only three generations of quarks and the absence of particles beyond the standard model (SM) [13]. This model dependence motivates alternative

inferences based on different sets of hypotheses. In particular, given that these three CKM elements connect the top quark with down-type quarks, it is natural to use events enriched in top quarks to set constraints on them. Two complementary approaches have been pursued by the Tevatron and LHC experiments to extract $|V_{tb}|$: the first method measures the branching fraction $\mathcal{B}(t \rightarrow Wb) = |V_{tb}|^2 / (|V_{td}|^2 + |V_{ts}|^2 + |V_{tb}|^2)$ in $t\bar{t}$ events [14–17]. The $\mathcal{B}(t \rightarrow Wb)$ measurement is sensitive to the CKM elements of interest through the decay vertex of the top quark, and can be turned into a measurement of the value of $|V_{tb}|$ only under the hypothesis of the unitarity of the 3×3 CKM matrix. The second method is based on the single top quark production cross section and is sensitive in principle through both the production and decay of the top quark. To disentangle the effects of the two vertices in past measurements at the Tevatron [18–27] and the LHC [2, 3, 5–10, 28, 29], $|V_{tb}|$ was extracted in the t channel by assuming that the values of $|V_{ts}|$ and $|V_{td}|$ are negligible. Some theoretical proposals have suggested the simultaneous extraction of the three CKM matrix elements from a combination of measurements of $\mathcal{B}(t \rightarrow Wb)$ and either inclusive [13, 30] or differential [31, 32] cross sections of single top quark production in the t channel. Other studies specifically address the determination of $|V_{td}|$ [31, 33] through a reliance on the reinterpretation of existing measurements, but they do not make use of full experimental detector simulations and do not exploit the discriminating power of multivariate analyses (see, for example, discussion in Ref. [34]).

The data used in this Letter come from pp collisions at $\sqrt{s} = 13$ TeV, corresponding to an integrated luminosity of 35.9 fb^{-1} and collected by the CMS experiment with triggers requiring either one muon or electron in the final state. We present the first direct and model-independent simultaneous measurement of $|V_{tb}|$, $|V_{td}|$, and $|V_{ts}|$, by considering their respective contributions to the top quark t -channel production and decay.

2 The CMS detector

The central feature of the CMS apparatus is a superconducting solenoid of 6 m internal diameter, providing a magnetic field of 3.8 T. Within the solenoid volume are a silicon pixel and strip tracker, a lead tungstate crystal electromagnetic calorimeter, and a brass and scintillator hadron calorimeter, each composed of a barrel and two endcap sections. Forward calorimeters extend the pseudorapidity (η) [35] coverage provided by the barrel and endcap detectors.

Events of interest are selected using a two-tiered trigger system [36]. The first level, composed of custom hardware processors, uses information from the calorimeters and muon detectors to select events. The second level, known as the high-level trigger, consists of a farm of processors running a version of the full event reconstruction software optimised for efficient processing. A more detailed description of the CMS detector, together with a definition of the coordinate system used and the relevant kinematic variables, can be found in Ref. [35].

3 Simulated samples

Monte Carlo (MC) event generators are used to simulate signal and background samples. Single top quark t -channel events are generated at next-to-leading-order (NLO) in quantum chromodynamics (QCD) with POWHEG 2.0 [37–39]. The four-flavour scheme [40] is used for events with the V_{tb} vertex in production, while the five-flavour scheme [41] is used for events with one V_{td} or V_{ts} vertex in production. Top quark decays are simulated with MADSPIN [42]. The $t\bar{t}$ background process [43], as well as double vector boson production [44, 45] (VV , where V stands for either a W or a Z boson), are generated with POWHEG 2.0. Associated top quark

and W boson production are simulated with POWHEG in the five-flavour scheme [46]. Single top quark s -channel events (t , s -ch) are simulated with MADGRAPH5_aMC@NLO 2.2.2 [47] at NLO. The value of the top quark mass used in the simulated samples is 172.5 GeV. For all samples PYTHIA 8.180 [48] with tune CUETP8M1 [49] is used to simulate the parton shower, quark hadronisation, and underlying event, except for $t\bar{t}$, where the tune CUETPM2T4 is used [50]. Simulated event samples with W and Z bosons in association with jets (W +jets, Z +jets) are generated using MADGRAPH5_aMC@NLO 2.2.2. For these processes, events with up to two additional partons emitted in the hard scattering are simulated, and the FxFx merging scheme [51] is used to avoid double counting with parton emissions generated in the parton showering. Simulated QCD multijet events, generated at LO with PYTHIA 8.180, are used to validate the estimation of this background with a technique based on control samples in data.

The default parametrisation of the parton distribution functions (PDFs) used in all simulations is NNPDF3.0 [52] at LO or NLO QCD, with the order matching that of the matrix element calculation. All generated events undergo a full simulation of the detector response according to the model of the CMS detector within GEANT4 [53]. Additional pp interactions within the same or nearby bunch crossings (pileup) are included in the simulation with the same distribution as observed in data. Except for the QCD multijet process, which is determined from a fit to data, all simulated samples are normalised to the expected cross sections.

4 Event selection and reconstruction

The signal event selection is based on final states where the top quark decays to a b , s , or d quark, and a W boson, which then decays to a lepton-neutrino pair. Events with exactly one muon or electron and at least two jets are considered in this analysis, as was done in the latest CMS single top quark cross section measurement [10]. The neutrino accompanying the lepton cannot be directly detected, and manifests itself in the detector as a measured momentum imbalance in the event. Depending on the CKM matrix element involved in the decay, the final state may include a jet from the hadronisation of either a b , s , or d quark. A jet recoiling against the top quark is present, and it is produced usually at low angle with respect to the beam axis. A third jet can stem from the second quark produced in the gluon splitting (as shown in Fig. 1(c)). The quark from gluon splitting generates a jet that usually has a softer transverse momentum (p_T) spectrum than that of the jet from the top quark decay products. Depending on the number of tWb vertices in the event process, one can have one jet coming from the hadronisation of a b quark (b jet) if the tWb vertex occurs in production or in decay but not in both, or two b jets if the tWb vertex occurs both in production and decay.

Events are retained for the offline analysis if they were selected online by requiring the presence of an isolated, high- p_T lepton: either a muon with $p_T > 24$ GeV or an electron with $p_T > 32$ GeV. From the sample of triggered events, only those with at least one primary vertex reconstructed from at least four tracks, with a longitudinal distance of less than 24 cm and a radial distance of less than 2 cm from the centre of the detector, are considered for the analysis. The candidate vertex with the largest value of summed physics-object p_T^2 is taken to be the primary pp interaction vertex. The physics objects are the jets, clustered using the jet-finding algorithm [54, 55] with the tracks assigned to candidate vertices as inputs, and the associated missing p_T (p_T^{miss}), taken as the magnitude of the negative vector sum of the \vec{p}_T^{miss} of those jets.

The particle-flow (PF) algorithm [56] is used to reconstruct and identify individual particles in the event using combined information from the subdetectors of the CMS experiment, allowing identification of muons, electrons, photons, and charged and neutral hadrons. After triggering, muons are considered for further analysis if they have $p_T > 26$ GeV and $|\eta| < 2.4$, while

electrons are required to have $p_T > 35$ GeV and $|\eta| < 2.1$. Additional isolation requirements are used to discriminate between prompt leptons and those coming from hadronic decays within jets, by defining I_{rel} , as the scalar sum of the p_T of charged hadrons, neutral hadrons, and photons divided by the p_T of lepton in a cone of $\Delta R = \sqrt{(\Delta\eta)^2 + (\Delta\phi)^2} = 0.4$ around the muon and 0.3 around the electron, where ϕ is the azimuthal angle in radians. The contribution of hadrons from pileup interactions is subtracted from the scalar sum with the techniques detailed in Refs. [57, 58]. The parameter I_{rel} is required to be less than 6.0% for muons, 5.9% for barrel electrons, and 5.7% for endcap electrons.

Jets are reconstructed using the anti- k_T clustering algorithm described in Refs. [54, 55] with a distance parameter of 0.4 on the collection of PF candidates. To be included, charged particle candidates must be closer along the z axis to the primary vertex than to any other vertex.

A correction to account for pileup interactions is estimated on an event-by-event basis using the jet area method described in Ref. [58], and is applied to the reconstructed jet p_T . Further jet energy corrections [59], derived from the study of dijet events and photon plus jet events in data, are applied. Two types of jets are defined: high- p_T jets are defined by requiring $|\eta| < 4.7$ and $p_T > 40$ GeV, and low- p_T jets are defined by requiring $|\eta| < 4.7$ and $20 < p_T < 40$ GeV.

Once the jets have been selected according to the above criteria, they can be further categorised using a b tagging discriminator variable in order to distinguish between jets stemming from the hadronisation of b quarks and those from the hadronisation of light partons. A multivariate (MVA) discriminator algorithm uses track-based lifetime information, together with secondary vertices inside the jet, to provide a MVA discriminator for b jet identification [60, 61]. For values of the discriminator above the chosen threshold, the efficiency of the tagging algorithm to correctly find b jets is about 45%, with a rate of 0.1% for mistagging light-parton jets [60, 61].

Events are divided into mutually exclusive ‘‘categories’’ according to the number of selected high- p_T jets and b -tagged high- p_T jets. In the following, categories are labelled as ‘‘ $n_j m_t$ ’’, referring to events with exactly n high- p_T jets, m of which are tagged as b jets, regardless of the number of low- p_T jets. The threshold on the jet momentum for high- p_T jets lessens the impact on the categorisation of additional jets coming from initial- or final-state radiation, which is fully simulated and taken into account in the modelling systematic uncertainties.

To reject events from QCD multijet background processes, a requirement on the transverse mass of the W boson of $m_T^W > 50$ GeV is imposed, where

$$m_T^W = \sqrt{(p_{T,\ell} + p_T^{\text{miss}})^2 - (p_{x,\ell} + p_x^{\text{miss}})^2 - (p_{y,\ell} + p_y^{\text{miss}})^2}. \quad (1)$$

Here, p_T^{miss} is defined as the magnitude of \vec{p}_T^{miss} , which is the negative of the vectorial \vec{p}_T sum of all the PF particles. The p_x^{miss} and p_y^{miss} quantities are the \vec{p}_T^{miss} components along the x and y axes, respectively, and $p_{T,\ell}$, $p_{x,\ell}$, and $p_{y,\ell}$ are the corresponding lepton momentum components in the transverse, x , and y directions.

To analyse the kinematics of single top quark production, the four-momentum of a top quark candidate is reconstructed from the decay products: leptons, neutrinos, and b jet candidates. The p_T of the neutrino can be inferred from p_T^{miss} . The longitudinal momentum of the neutrino, $p_{z,\nu}$, is calculated assuming energy-momentum conservation at the $W\ell\nu$ vertex and constraining the W boson mass to $m_W = 80.4$ GeV [12]:

$$p_{z,\nu}^\pm = \frac{\Lambda p_{z,\ell}}{p_{T,\ell}^2} \pm \frac{1}{p_{T,\ell}^2} \sqrt{\Lambda^2 p_{z,\ell}^2 - p_{T,\ell}^2 (p_\ell^2 p_{T,\nu}^2 - \Lambda^2)}, \quad (2)$$

where

$$\Lambda = \frac{m_W^2}{2} + \vec{p}_{T,\ell} \cdot \vec{p}_T^{\text{miss}}, \quad (3)$$

and $p_\ell^2 = p_{T,\ell}^2 + p_{z,\ell}^2$ denotes the square of the lepton momentum. In most of the cases, this leads to two real solutions for $p_{z,\nu}$ and the solution with the smallest absolute value is chosen [21, 23]. For some events, the discriminant in Eq. (2) becomes negative, leading to complex solutions for $p_{z,\nu}$. In this case, the imaginary component is eliminated by modification of $p_{x,\nu}$ and $p_{y,\nu}$ so that $m_T^W = m_W$, while still respecting the m_W constraint. This is achieved by requiring the determinant, and thus the square-root term in Eq. (2), to equal zero. This condition gives a quadratic relation between $p_{x,\nu}$ and $p_{y,\nu}$ with two possible solutions and one remaining degree of freedom. The solution is chosen by finding the $\vec{p}_{T,\nu}$ that has the minimum vectorial distance from \vec{p}_T^{miss} in the $p_x^{\text{miss}} - p_y^{\text{miss}}$ plane.

A reconstructed top quark candidate is defined by associating one jet with an accompanying W boson, and the respective top quark four-momentum is evaluated as described above. For each of the signal categories selected, multiple top quark candidates can be defined in the same category, depending on the hypothesis for the origin of the jet in the event.

5 Signal description and event categorisation

The predicted branching fractions of top quarks to d, s, and b quarks can be written as a function of the overall magnitude of $\mathcal{B}(t \rightarrow Wq) = |V_{tq}|^2 / (|V_{td}|^2 + |V_{ts}|^2 + |V_{tb}|^2)$. The values of $|V_{tq}|$ and $\mathcal{B}(t \rightarrow Wq)$ used to derive the initial normalisation of signal processes are taken from Ref. [12], and shown in Table 1.

Table 1: Values of the third-row elements of the CKM matrix inferred from low-energy measurements, taken from Ref. [12], with the respective values of the top quark decay branching fractions. The q in $|V_{tq}|$ and $\mathcal{B}(t \rightarrow Wq)$ in the first column refers to b, s, and d quarks, according to the quark label shown in the header row.

Quark	b	s	d
$ V_{tq} $	$0.999119^{+0.000024}_{-0.000012}$	$0.04108^{+0.00030}_{-0.00057}$	$0.008575^{+0.000076}_{-0.000098}$
$\mathcal{B}(t \rightarrow Wq)$	$0.998239^{+0.000048}_{-0.000024}$	$0.0016876^{+0.0000025}_{-0.0000047}$	$0.000074^{+0.000013}_{-0.000017}$

The quantities reported in Table 1 come from low-energy measurements that assume unitarity in the CKM matrix and no new loops in the relevant Feynman diagrams. This analysis will relax such assumptions and present different scenarios for interpretation of the provided results.

The signatures for t -channel processes involving V_{tb} , V_{td} , and V_{ts} either in production or decay differ in three aspects: the number of reconstructed b-tagged jets, the features of the jet involved in the reconstruction of the correct top quark candidate, and the kinematic features of the events as a result of different PDF contributions to production modes involving a b, s, or d quark. Henceforth, the t -channel process involving V_{tb} in both production and decay will be referred to as $ST_{b,b}$, while t -channel processes involving V_{tb} in only production or decay will be referred to as $ST_{b,q}$ and $ST_{q,b}$, respectively. The signal channels and their corresponding cross sections times branching fractions from simulation are reported in Table 2. The cross sections are evaluated at NLO in the five-flavour scheme using POWHEG for $\sigma_{t\text{-ch},d}$, $\sigma_{t\text{-ch},s}$, and with HATHOR [62] for $\sigma_{t\text{-ch},b}$.

Multiple categories are defined in order to extract the contribution of the different t -channel processes, while at the same time discriminating against the background processes, mainly $t\bar{t}$

Table 2: For each of the production and decay vertices, the cross section times branching fraction for the corresponding signal process from simulation. The uncertainties shown include those from the factorisation and renormalisation scales, the PDFs, and any experimental uncertainties, where appropriate.

Production	Decay	Cross section \times branching fraction (pb)
tWb	tWb	217.0 ± 8.4
tWb	(tWs + tWd)	0.41 ± 0.05
tWd	tWb	0.102 ± 0.015
tWs	tWb	0.92 ± 0.11

and W +jets production. The majority of t -channel events populate categories with 2 or 3 jets, as defined above. The main backgrounds arise from $t\bar{t}$ (all categories), W +jets (in the 2j1t and 3j1t categories), and QCD multijet (in the 2j1t category) processes. The signal processes taken into consideration give different contributions to the three categories, and it is possible to identify the most sensitive categories with respect to each process based on the respective signatures, as summarised in Table 3. The physics motivations leading to this strategy are described below.

Events from strong interaction $t\bar{t}$ production, where one top quark decays through the tWd or tWs vertex ($t\bar{t}_{b,q}$), populate the 2j1t and 3j1t categories. Their small contribution to the $t\bar{t}$ yield in such categories is covered by the b -tagging uncertainty. Their signature in those categories is also found to be indistinguishable, within systematic uncertainties, from that of $t\bar{t}$ when each top quark decays through the tWb vertex and one b jet does not pass either the kinematic or b tagging requirements. For those reasons, all top quark decay modes of $t\bar{t}$ pairs are treated as a single background source.

Table 3: For each category, the corresponding signal process, the cross section times branching fraction expression, and the specific Feynman diagram from Fig. 1 are shown.

Category	Enriched in	Cross section \times branching fraction	Feynman diagram
2j1t	$ST_{b,b}$	$\sigma_{t\text{-ch},b} \mathcal{B}(t \rightarrow Wb)$	1a
3j1t	$ST_{b,q}, ST_{q,b}$	$\sigma_{t\text{-ch},b} \mathcal{B}(t \rightarrow Wq), \sigma_{t\text{-ch},q} \mathcal{B}(t \rightarrow Wb)$	1b, 1c, 1d
3j2t	$ST_{b,b}$	$\sigma_{t\text{-ch},b} \mathcal{B}(t \rightarrow Wb)$	1a

The discrimination between the three signals $ST_{b,q}$, $ST_{q,b}$, and $ST_{b,b}$ is based on three characteristics. First, for $ST_{b,q}$ events, only a single b quark is present in the final state stemming from gluon splitting, thus resulting in a low-energy b -tagged jet, while the jet coming from the top quark decay is usually not b tagged. For $ST_{q,b}$ events, a single b -tagged jet is produced in the top quark decay, and additional jets from gluon splitting are usually not b tagged. Both $ST_{q,b}$ and $ST_{b,q}$ processes therefore differ from $ST_{b,b}$ by having a single b quark in the final state, as opposed to two for the latter process. However, this feature can only be exploited when the jet from gluon splitting is energetic enough to be reconstructed. Second, further discrimination is achieved by exploiting the features of the reconstructed top quark candidates. The kinematic and angular properties of the decay products exhibit significant differences depending on whether the correct jet is chosen, or if the jet that originated from the quark produced in the gluon splitting is used. For $ST_{b,q}$ events, the top quark reconstructed with the correct jet assignment usually does not use the b -tagged jet in the event, while for $ST_{b,b}$ and $ST_{q,b}$, the top quark candidate is reconstructed by using the b -tagged jet in the majority of cases. It is therefore possible to differentiate between the $ST_{b,b}$ and $ST_{b,q}$ processes by comparing the features of top quark candidates reconstructed with or without b -tagged jets. Finally, different PDFs are involved in $ST_{b,b}$ and $ST_{q,b}$ processes, the latter drawing contributions from valence d quarks as well. Therefore, the kinematic properties of final-state particles may differ from the other

channels. The second characteristic, related to the correctness of the top quark reconstruction hypothesis, proves to be the strongest amongst the three mentioned criteria. While the $ST_{b,q}$ and the $ST_{b,b}$ processes can be differentiated by using this characteristic, the $ST_{q,b}$ and the $ST_{b,b}$ productions cannot, because their final-state signatures exhibit the same features.

The 2j1t category is populated by events that depend on V_{tb} in both production and decay, where the single reconstructed b jet comes in the majority of cases (85%) from top quark decays, and for the remaining cases from the second b jet from gluon splitting. This means that the jet from the second b quark fails either the jet p_T requirement or the b tag requirement, or both. Events coming from a process for which V_{td} or V_{ts} are involved, either in production or in decay, populate this category as well, with either the b-tagged jet coming from top quark decay or the secondary b quark from gluon splitting.

For t -channel signal events from all four processes in Fig. 1, the most distinctive features that allow the discrimination against backgrounds in the 2j1t category rely on the fact that the second jet stems from the recoiling quark. For this reason the non-b-tagged jet is not used for the top quark reconstruction. This category is the one where the highest discrimination power for $ST_{b,b}$ against backgrounds is achieved by making use of the features of the top quark decay products, such as the reconstructed top quark mass and m_T^W , and of the recoiling jet. However, the discrimination power with respect to other t -channel mechanisms is poor since jets from gluon splitting are typically not energetic enough to pass the p_T threshold, making it impossible to reconstruct two different top quark candidates.

The 3j1t category is also populated by all t -channel processes of interest, but it differs from 2j1t in the fact that it accommodates events in which the jet from gluon splitting has a higher p_T on average. For both the 2j1t and 3j1t categories, when the top quark decays through tWd,s vertices, the jet coming from the top quark usually does not pass the b tagging requirement since it stems from the hadronisation of a light quark. In all other cases, this jet passes the b tagging requirement, given the efficiency of the tagging algorithm.

The 3j1t category is enriched in t -channel events by requiring $|\eta_j| > 2.5$, where η_j is the pseudorapidity of the most forward jet. The two jets other than the most forward one are used to reconstruct the two top quark candidates. If the event is from the $ST_{b,q}$ process, the b-tagged jet in the 3j1t category will stem from gluon splitting, and the additional jet will have a higher chance of being the one coming from the top quark decay to an s or d quark. Variables of interest in this case are constructed by making use of the b jet and the least forward jet of the remaining two, referred to as the extra jet. Such variables include the invariant mass of the lepton plus jet system (either the b jet or the extra jet), and several top quark kinematic variables constructed using a combination of the extra jet, the lepton, and p_T^{miss} .

In both the 2j1t and the 3j1t categories, m_T^W is also used to discriminate between the QCD multijet background and other processes. An event category depleted of QCD multijet background is defined by adding the requirement $m_T^W > 50 \text{ GeV}$. Figure 2 shows the m_T^W distribution from data and simulations in the 2j1t and 3j1t categories for the muon (upper plots) and electron (lower plots) channels, where the QCD multijet background is normalised to the result of the fit.

In the 3j2t category, there are two b jets, one produced from the top quark decay and another from gluon splitting. Both b jets are used to reconstruct a top quark candidate and its corresponding variables. In this case, the $m_T^W > 50 \text{ GeV}$ requirement is unnecessary since the QCD multijet contamination is negligible and the dominant background process is $t\bar{t}$. No requirement on η_j is needed either since the category is dominated by the $ST_{b,b}$ process and the

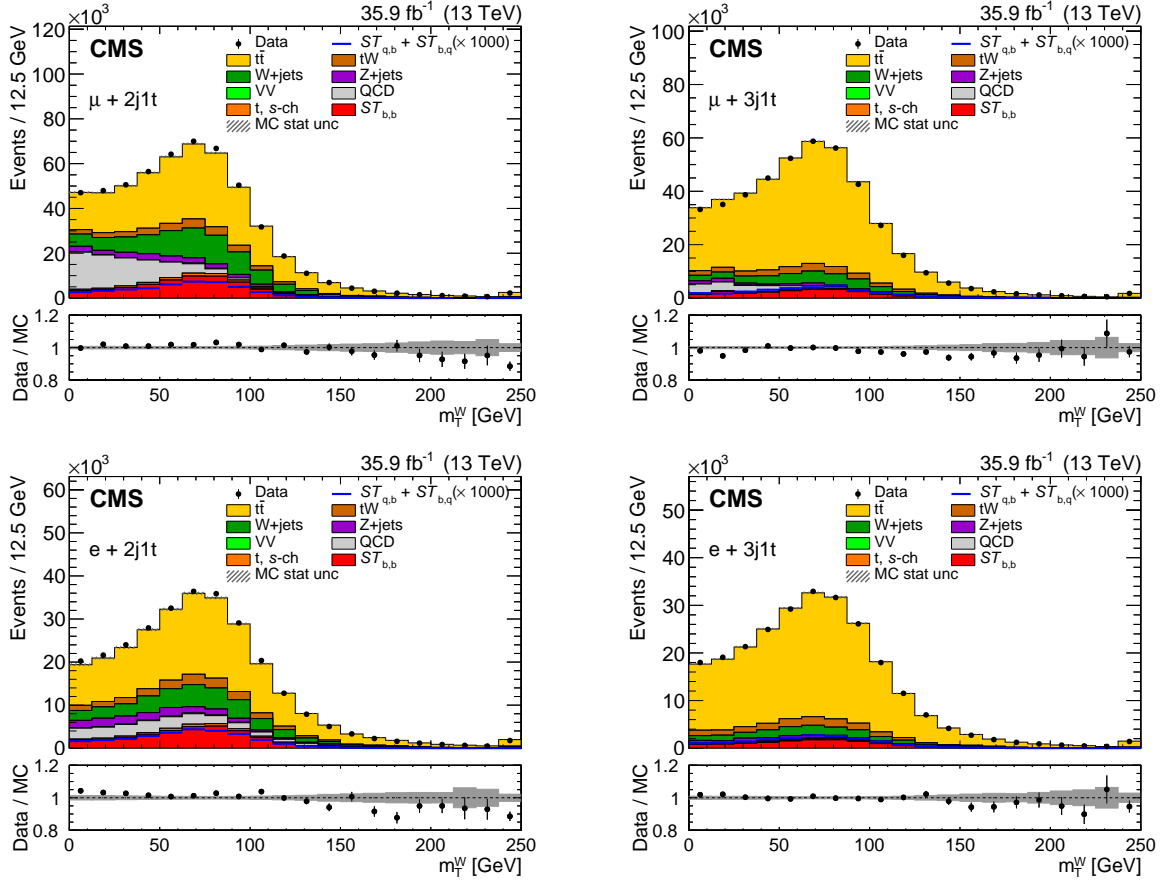


Figure 2: The m_T^W distribution from data (points) and simulation (shaded histograms) in the 2j1t (left) and 3j1t (right) categories for the muon (upper) and electron (lower) channels. The vertical lines on the points and the hatched bands show the experimental and MC statistical uncertainties, respectively. The expected distribution from the $ST_{q,b} + ST_{b,q}$ processes (multiplied by a factor of 1000) is shown by the solid blue line. The lower panels show the ratio of the data to the MC prediction.

combinatorial top quark background is small.

Multivariate analyses are then performed by using boosted decision trees (BDT) in order to obtain appropriate discriminating variables, henceforth referred to as BDT discriminators, in the three categories, for both muons and electrons. The processes used as signal or background in the training are the following:

- In the 2j1t category, the single top quark $ST_{b,b}$ process is considered as signal and $t\bar{t}$ and W+jets processes as background.
- In the 3j1t category, the single top quark $ST_{q,b}$ process is considered as signal and the $ST_{b,b}$, $t\bar{t}$, and W+jets processes as background.
- In the 3j2t category, the single top quark $ST_{b,b}$ process is considered as signal and $t\bar{t}$ as background.

The variables used in the 2j1t category training are: the $|\eta|$ of the non-b-tagged jet, the reconstructed top quark mass, the cosine of the angle between the W boson momentum in the top quark rest frame and the momentum of the lepton in the W boson rest frame, the cosine of the polarisation angle defined as the angle between the direction of the lepton and the light-quark

momenta in the top quark rest frame, the invariant mass of the lepton and b-tagged jet system, and the invariant mass of the lepton and forward jet system.

The variables used in the 3j1t category training are: the $|\eta|$ of the most forward non-b-tagged jet, the mass of the top quark when it is reconstructed with the b-tagged jet (b-top quark), the cosine of the angle between the W boson momentum in the b-top quark rest frame and the momentum of the lepton in the W boson rest frame, the cosine of the polarisation angle defined as the angle between the direction of the lepton and the light-quark momenta in the b-top quark rest frame, p_T^{miss} , m_T^W , the invariant mass of the lepton and b-tagged jet system, the invariant mass of the lepton and extra jet system, the invariant mass of the lepton and forward jet system, the number of low- p_T jets, the mass of the top quark when it is reconstructed with the non-b-tagged jet (non-b-top quark), the cosine of the angle between the W boson momentum in the non-b-top quark rest frame and the momentum of the lepton in the W boson rest frame, the cosine of the polarisation angle defined as the angle between the direction of the lepton and the light-quark momenta in the non-b-top quark rest frame, and the value of the MVA b tagger discriminator when applied to the non-b-tagged jet.

The variables used in the 3j2t category training are: the $|\eta|$ of the non-b-tagged jet, the mass of the top quark when it is reconstructed with the highest- p_T b-tagged jet (leading top quark), the cosine of the angle between the W boson momentum in the leading top quark rest frame and the momentum of the lepton in the W boson rest frame, the cosine of the polarisation angle defined as the angle between the direction of the lepton and the light-quark momenta in the leading top quark rest frame, p_T^{miss} , m_T^W , the invariant mass of the lepton and the highest- p_T b-tagged jet system, the invariant mass of the lepton and lower- p_T b-tagged jet system, the invariant mass of the lepton and light-jet system, the number of low- p_T jets, the mass of the top quark when it is reconstructed with the lower- p_T b-tagged jet (non-leading top quark), the cosine of the angle between the W boson momentum in the non-leading top quark rest frame and the momentum of the lepton in the W boson rest frame, the cosine of the polarisation angle defined as the angle between the direction of the lepton and the light-quark momenta in the non-leading top quark rest frame, and the difference in η between the two b-tagged jets.

Figures 3–5 show the distributions of the most discriminating variables in the 2j1t, 3j1t, and 3j2t categories, respectively.

6 Systematic uncertainties

Several sources of systematic uncertainties are considered in the analysis, divided in two groups depending on the treatment: uncertainties labelled as “profiled” are treated as nuisance parameters and profiled in the fit procedure described in Section 7, while those labelled as “nonprofiled” are estimated as the difference between the result of the fit procedure by varying the systematic scenario. These latter uncertainties include the sources related to the modelling of the signal process, which cannot be constrained from the measurement since they apply to the full phase space and not only to the region in which the measurement is performed. Also included are the jet energy scale and resolution uncertainties, which play a major role in events featuring hadronic activity in the high-pseudorapidity region of the detector. They are also intertwined with the uncertainties in the modelling of the hadronisation and cause a larger uncertainty in the signal acceptance, which was not the case for previous measurements [10, 11]. For these reasons, a more conservative approach is preferred and these uncertainties are not profiled in the fit.

The impact of nonprofiled uncertainties is determined by repeating the analysis using varied

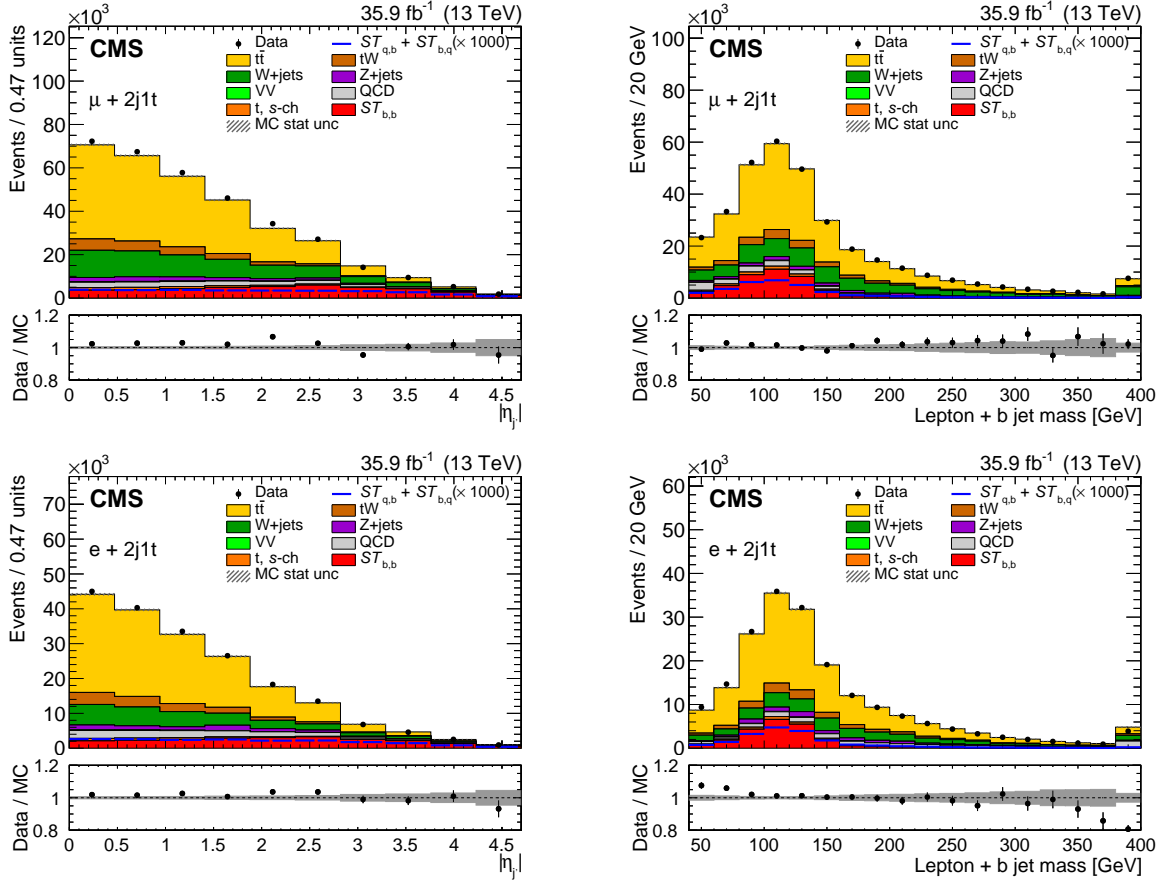


Figure 3: Distributions of the two most discriminating variables from data (points) and simulation (shaded histograms) in the 2j1t category: the $|\eta_j|$ of the non-b-tagged jet η_j (left) and the invariant mass of lepton and b jet momenta system (right), shown for the muon (upper) and electron (lower) channels, respectively. The vertical lines on the points and the hatched bands show the experimental and MC statistical uncertainties, respectively. The expected distribution from the $ST_{q,b} + ST_{b,q}$ processes (multiplied by a factor of 1000) is shown by the solid blue line. The lower panels show the ratio of the data to the MC prediction.

templates according to the systematic uncertainty sources under study in the fit, instead of the nominal templates. The uncertainty due to a certain source is then taken as half the difference between the results for up and down variations of the effect. In the following, the different uncertainty sources that are considered in the analysis are briefly described. For the sake of simplicity and better readability, they are grouped into profiled and nonprofiled uncertainties.

Profiled uncertainties

- *Limited size of simulated event samples:* The statistical uncertainty due to the limited size of the simulated event samples is evaluated for each bin with the Barlow–Beeston “light” method [63, 64].
- *Lepton trigger and reconstruction:* Single-muon and single-electron trigger and reconstruction efficiencies are estimated with a “tag-and-probe” method [65] from Drell–Yan events with the dilepton invariant mass in the Z boson peak.
- *Pileup:* The uncertainty in the average expected number of pileup interactions is propagated as a source of systematic uncertainty by varying the total pp inelastic cross section by $\pm 4.6\%$ [66].

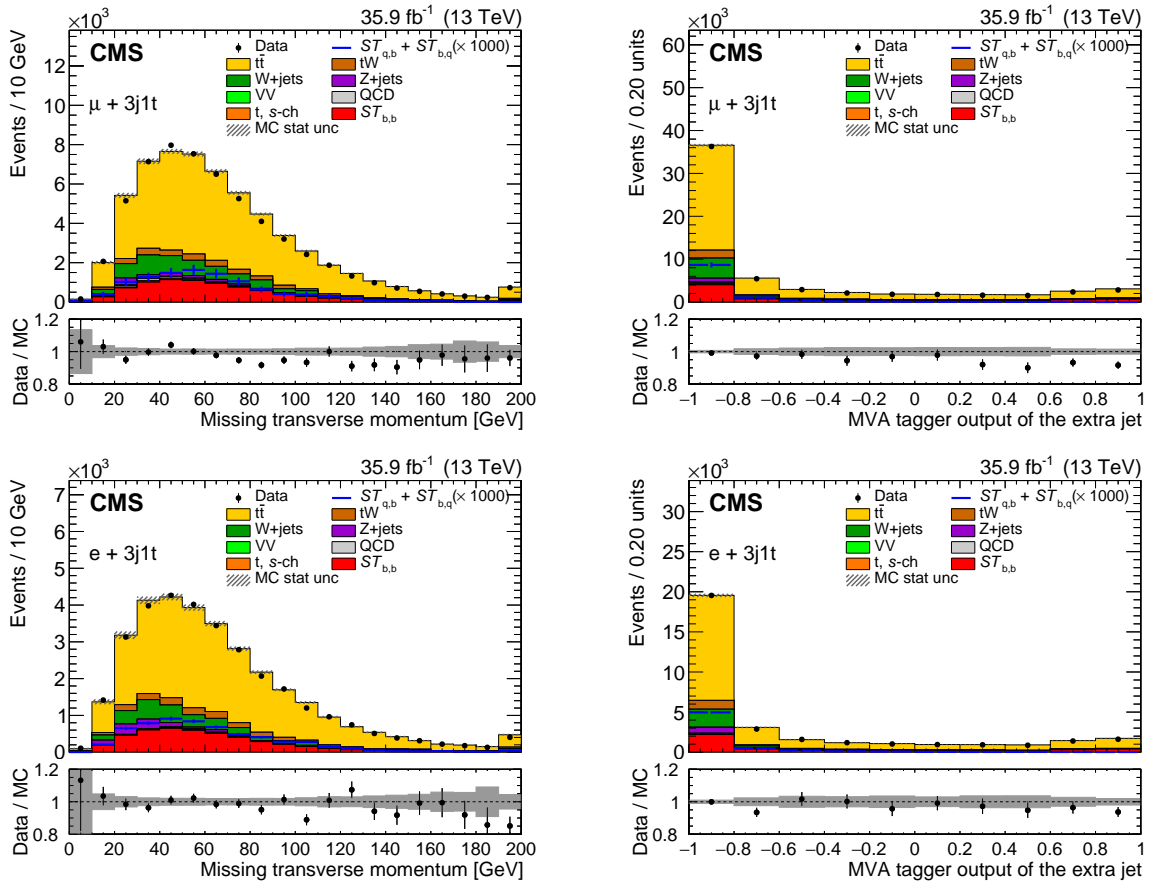


Figure 4: Distributions of the two most discriminating variables from data (points) and simulation (shaded histograms) in the 3j1t category: the p_T^{miss} in the transverse plane (left) and the value of the MVA b tagger discriminator when applied to the extra jet (right) are shown for the muon (upper) and electron (lower) channels, respectively. The vertical lines on the points and the hatched bands show the experimental and MC statistical uncertainties, respectively. The expected distribution from the $ST_{q,b} + ST_{b,q}$ processes (multiplied by a factor of 1000) is shown by the solid blue line. The lower panels show the ratio of the data to the MC prediction.

- *$t\bar{t}$ modelling*: The following uncertainty sources cover potential mismodelling of the $t\bar{t}$ process. Their effect is considered on both the acceptance and the cross section.
 - *$t\bar{t}$ renormalisation and factorisation scale uncertainties (μ_R/μ_F)*: The uncertainties caused by variations in the renormalisation and factorisation scales are considered by reweighting the BDT response distributions with different combinations of doubled/halved renormalisation and factorisation scales with respect to the nominal value of 172.5 GeV.
 - *Matching of matrix element and parton shower (ME-PS matching)*: The parameter that controls the matching between the matrix element level calculation and the parton shower, and that regulates the high- p_T radiation in the simulation is varied within its uncertainties.
 - *Initial- and final-state radiation*: The impact of variations in the initial-state and final-state radiation is studied by comparing the nominal sample with dedicated $t\bar{t}$ samples.
 - *Underlying event*: The effect of uncertainties in the modelling of the underlying event is studied by comparing the nominal sample with dedicated

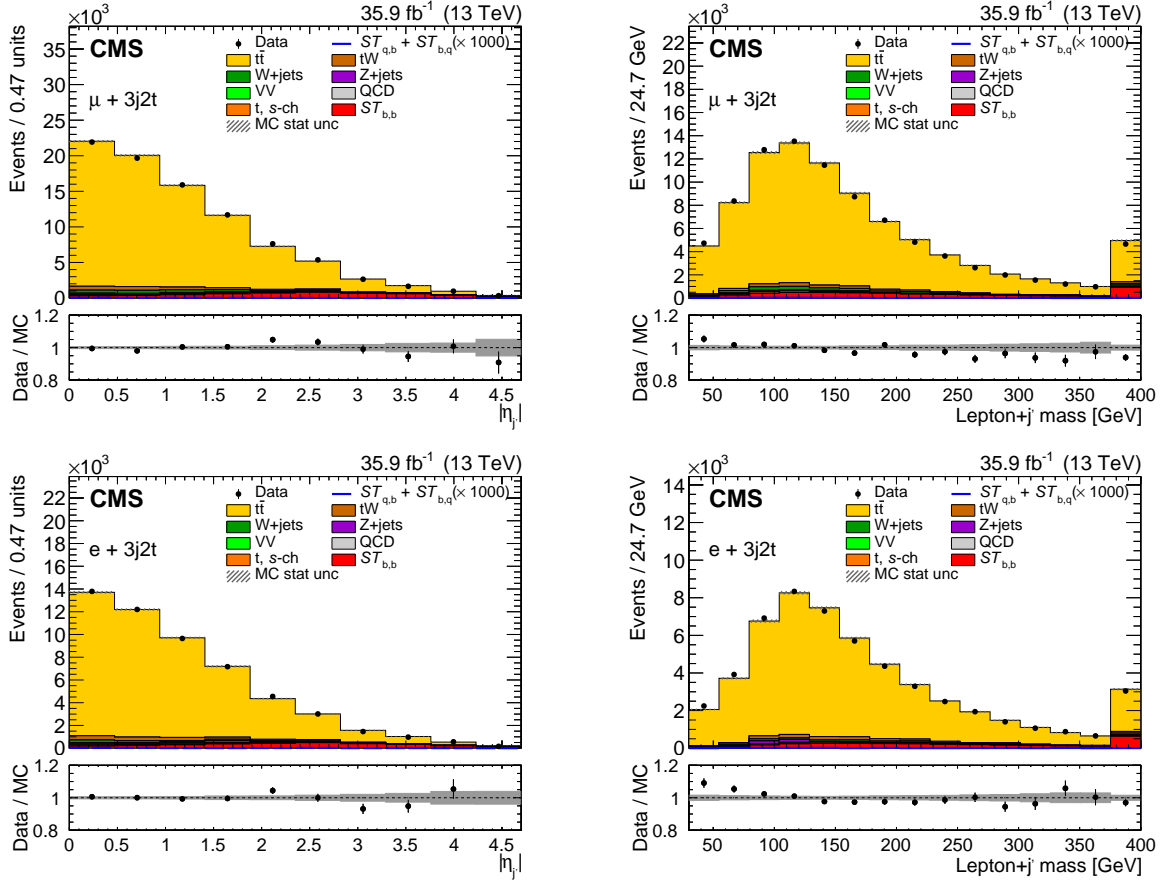


Figure 5: Distributions of the two most discriminating variables from data (points) and simulation (shaded histograms) in the 3j2t category: the $|\eta_j|$ of the non-b-tagged jet η_j (left) and the invariant mass of lepton and non-b-tagged jet system (right) are shown for the muon (upper) and electron (lower) channels, respectively. The vertical lines on the points and the hatched bands show the experimental and MC statistical uncertainties, respectively. The expected distribution from the $ST_{q,b} + ST_{b,q}$ processes (multiplied by a factor of 1000) is shown by the solid blue line. The lower panels show the ratio of the data to the MC prediction.

$t\bar{t}$ samples.

- *QCD multijet background process normalisation:* The QCD multijet background yield is assigned a 50% uncertainty, which is chosen conservatively to be much larger than the uncertainty from the m_T^W fit.
- *W+jets composition:* A separate uncertainty is dedicated to the fraction of W+jets events where the forward jet is generated by the parton showering.
- *Other backgrounds μ_R/μ_F :* In addition to $t\bar{t}$, the uncertainties due to variations in the renormalisation and factorisation scales are studied for the tW and W+jets processes by reweighting the distributions with weights corresponding to different combinations of halved or doubled factorisation and renormalisation scales. The effect is estimated for each process separately.
- *PDF for background processes:* The uncertainty due to the choice of PDF is estimated using reweighted histograms derived from all PDF sets of NNPDF 3.0 [67].
- *b tagging:* The uncertainties in the b tagging and mistagging efficiency measurements are split into different components and propagated to the efficiency of tagging

b jets.

Nonprofiled uncertainties

- *Luminosity*: The integrated luminosity is known with a relative uncertainty of $\pm 2.6\%$ [68].
- *Jet energy scale (JES)*: All reconstructed jet four-momenta in simulated events are simultaneously varied according to the η - and p_T -dependent uncertainties in the JES [59]. This variation in jet four-momenta is also propagated to p_T^{miss} .
- *Jet energy resolution (JER)*: A smearing is applied to account for the difference in the JER between simulation and data [59], and its uncertainty is estimated by increasing or decreasing the resolutions by their uncertainties.
- *Signal modelling*: The following uncertainty sources cover potential mismodelling of the single top quark t -channel signal processes. The effect of those uncertainties on the acceptance, and not on the cross section, is considered. In the fit procedure, the uncertainties are not considered as nuisance parameters in the fit but evaluated by repeating the full analysis using samples of simulated signal events that feature variations in the modelling parameters covering the systematic uncertainty sources under study.
 - *Signal μ_R/μ_F* : The uncertainties caused by variations in the renormalisation and factorisation scales are considered by reweighting the BDT response distributions according to weights corresponding to doubling/halving the nominal values of the scales [40, 41].
 - *Matching of matrix element and parton shower (ME-PS matching)*: The parameter that controls the matching between the matrix element level calculation and the parton shower, and that regulates the high- p_T radiation in the simulation is varied within its uncertainties.
 - *Parton shower factorisation scale*: The renormalisation scales of the initial- and final-state parton shower are varied by factors of two and one half with respect to the nominal value of 172.5 GeV.
 - *PDF for signal process*: The uncertainty due to the choice of PDF is estimated using reweighted histograms derived from all PDF sets of NNPDF 3.0. The measurements in the following report only the experimental uncertainties, while the uncertainties on the predicted cross sections are reported in Table 2. Effects on the fit due to correlation between PDFs are considered negligible.

7 Fit procedure

The three CKM matrix elements are extracted by measuring the production cross sections and branching fractions of single top quark t -channel processes that depend on V_{tb} , V_{td} , and V_{ts} in production and decay. The vast majority of single top quark t -channel events come from the $ST_{b,b}$ process, while $ST_{b,q}$ and $ST_{q,b}$ constitute subdominant production mechanisms. The $t\bar{t}_{b,q}$ contribution is taken into account in the background estimation.

The fit procedure is divided into two steps. In the first step, a maximum likelihood (ML) fit to the m_T^W distribution is performed separately for the 2j1t and 3j1t categories in order to extract the QCD multijet contribution. The QCD multijet normalisation and the relative uncertainty are extrapolated to the QCD multijet depleted categories and used as an input to the second

step. In the second step, in order to discriminate between $ST_{b,b}$, $ST_{q,b}$, and $ST_{b,q}$, the multivariate discriminators described in Section 5 are used in a simultaneous ML fit to the three event categories, while the QCD multijet prior uncertainty and central value are taken from the first step.

The t -channel single top quark signals are parametrised with a flat prior representing the coupling strength, and all systematic uncertainties are treated as described in Section 6. The smaller background yields are allowed to vary in the fit, along with the respective scale uncertainties. The QCD multijet background is fitted with a flat prior nuisance, while $t\bar{t}$ and W +jets backgrounds are left floating within the respective systematic uncertainties. The t -channel $ST_{b,q}$ and $t\bar{t}_{b,q}$ processes do not distinguish between topologies depending on V_{td} or V_{ts} in the decay, while $ST_{q,b}$ is sensitive to the different PDFs contributing to the processes. Figure 6 shows the distributions after the fit procedure has been applied for the muon (left) and the electron (right) channels. The partial and total contributions of the profiled and nonprofiled uncertainties are given in Table 4.

Table 4: The sources and relative values in percent of the systematic uncertainty in the measurement of the $ST_{b,b}$ cross section. The uncertainties are broken up into profiled and nonprofiled sources.

Treatment	Uncertainty	$\Delta\sigma_{ST_{b,b}}/\sigma$ (%)
Profiled	Lepton trigger and reconstruction	0.50
	Limited size of simulated event samples	3.13
	$t\bar{t}$ modelling	0.66
	Pileup	0.35
	QCD background normalisation	0.08
	W +jets composition	0.13
	Other backgrounds μ_R/μ_F	0.44
	PDF for background processes	0.42
	b tagging	0.73
	Total profiled	3.4
Nonprofiled	Integrated luminosity	2.5
	JER	2.8
	JES	8.0
	PDF for signal process	3.8
	Signal μ_R/μ_F	2.4
	ME-PS matching	3.7
	Parton shower scale	6.1
Total nonprofiled	11.5	
Total uncertainty	12.0	

8 Results and interpretation

The contributions of each of the three CKM matrix elements to the different $ST_{b,b}$, $ST_{b,q}$, and $ST_{q,b}$ cross sections, extracted from the fit procedure, are considered. In the SM, top quarks only decay to W bosons plus b , s , or d quarks, and their branching fractions are proportional to the magnitude squared of the respective matrix element, as given in Table 2. The fit results are given in terms of two signal strength parameters: the first, μ_b , refers to the $ST_{b,b}$ process,

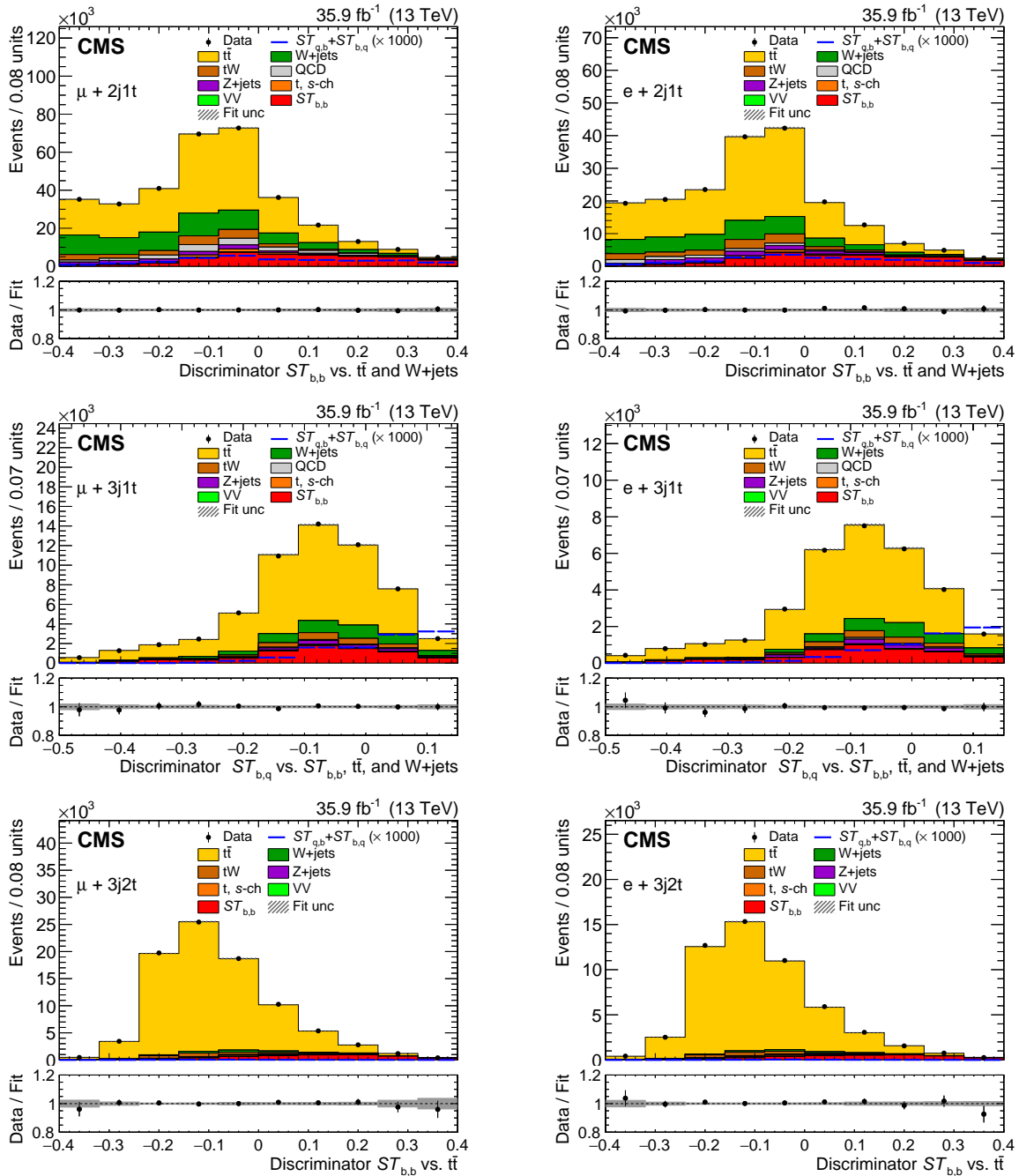


Figure 6: Distribution of the multivariate discriminators, comparing data to simulation normalised after the fit procedure, for the muon channel on the left and for the electron channel on the right, for $2j1t$ (upper), $3j1t$ (middle), and $3j2t$ (lower). The vertical lines on the points and the hatched bands show the experimental and fit uncertainties, respectively. The expected distribution from the $ST_{q,b} + ST_{b,q}$ processes (multiplied by a factor of 1000) is shown by the solid blue line. The lower panels show the ratio of the data to the fit.

and the second, μ_{sd} , to the sum of the $ST_{q,b}$ and $ST_{b,q}$ contributions.

By neglecting terms proportional to $|V_{td}|^4$, $|V_{ts}|^4$, the $ST_{q,b}$ term can be written as proportional to $|V_{td}|^2 + |V_{ts}|^2$, with a contribution of order 5% that depends on $|V_{td}|^2/|V_{ts}|^2$. We consider variations on the latter contribution as negligible in the analysis. These assumptions can be justified because of the hierarchy observed in the first two rows of the CKM matrix. The signal strengths thus become:

$$\begin{aligned}\mu_b &= \frac{\sigma_{t\text{-ch},b}^{\text{obs}} \mathcal{B}(t \rightarrow Wb)^{\text{obs}}}{\sigma_{t\text{-ch},b} \mathcal{B}(t \rightarrow Wb)} \\ \mu_{sd} &= \frac{\sigma_{t\text{-ch},b}^{\text{obs}} \mathcal{B}(t \rightarrow Ws, d)^{\text{obs}} + \sigma_{t\text{-ch},s,d}^{\text{obs}} \mathcal{B}(t \rightarrow Wb)^{\text{obs}}}{\sigma_{t\text{-ch},b} \mathcal{B}(t \rightarrow Ws, d) + \sigma_{t\text{-ch},s,d} \mathcal{B}(t \rightarrow Wb)},\end{aligned}\quad (4)$$

where $\mathcal{B}(t \rightarrow Ws, d)$ is the branching fraction for a top quark to decay to a W boson and either an s or d quark. Henceforth, the ‘‘obs’’ label will refer to the measured value of a quantity, and the absence of this label will mean the expected value. Equation (4) shows that the signal strengths are the ratios of the measured value of a quantity to the expected value.

One can write Eq. (4) more generally in terms of the top quark decay amplitudes or partial widths. We factorise out the modulus of the matrix element from the partial width for each quark. Thus, the top quark partial width to Wq can be written as $\Gamma_q = \tilde{\Gamma}_q |V_{tq}|^2$, where $\tilde{\Gamma}_q$ is the top quark partial width for $|V_{tq}| = 1$. We further assume that $\tilde{\Gamma}_q = \tilde{\Gamma}_b$, i.e. that any differences other than the CKM elements are negligible. Using this and the total width Γ_t of the top quark, we can write Eq. (4) as:

$$\begin{aligned}\mu_b &= \frac{|V_{tb}|_{\text{obs}}^4 \tilde{\Gamma}_q^{\text{obs}} \Gamma_t}{|V_{tb}|^4 \tilde{\Gamma}_q \Gamma_t^{\text{obs}}} \\ \mu_{sd} &= \frac{|V_{tb}|_{\text{obs}}^2 (|V_{ts}|_{\text{obs}}^2 + |V_{td}|_{\text{obs}}^2) \tilde{\Gamma}_q^{\text{obs}} \Gamma_t}{|V_{tb}|^2 (|V_{ts}|^2 + |V_{td}|^2) \tilde{\Gamma}_q \Gamma_t^{\text{obs}}}.\end{aligned}\quad (5)$$

The first fit extracts the signal strengths μ_b and μ_{sd} , whose values can be interpreted under different model assumptions. The signal strengths obtained are:

$$\begin{aligned}\mu_b &= 0.99 \pm 0.03 \text{ (stat+prof)} \pm 0.12 \text{ (nonprof)} \\ \mu_{sd} &< 87 \text{ at 95\% confidence level (CL)},\end{aligned}\quad (6)$$

with a correlation factor of $\rho_{\mu_b, \mu_{sd}} = -0.25$. The first uncertainty on μ_b is the combination of the statistical and profiled systematic uncertainties, while the second is due to the nonprofiled systematic components. The upper limit on μ_{sd} takes into account both profiled and nonprofiled systematic uncertainties.

In the following, we describe the signal extraction using the values of the CKM elements directly as parameters in the fit and applying constraints from the SM scenario and then two possible beyond-the-SM (BSM) extensions.

8.1 Measurement in the SM scenario

One can simplify Eq. (4) by assuming the SM unitarity constraint $|V_{tb}|^2 + |V_{td}|^2 + |V_{ts}|^2 = 1$. The fit is repeated, taking $|V_{tb}|$ as the single free parameter and replacing $|V_{td}|^2 + |V_{ts}|^2$ with

$1 - |V_{tb}|^2$. In this case, Eq. (4) becomes:

$$\begin{aligned}\mu_b &= \frac{|V_{tb}|_{\text{obs}}^4}{|V_{tb}|^4} \\ \mu_{\text{sd}} &= \frac{|V_{tb}|_{\text{obs}}^2 (1 - |V_{tb}|_{\text{obs}}^2)}{|V_{tb}|^2 (1 - |V_{tb}|^2)}.\end{aligned}\tag{7}$$

The fit is only allowed to return values of $|V_{tb}| \leq 1$, and the constraint $|V_{td}|^2 + |V_{ts}|^2 = 1 - |V_{tb}|^2$ is imposed. Because of these constraints, Gaussian behaviour of the uncertainties cannot be assumed. Instead, pseudo-experiments are generated to evaluate the impact of nonprofiled uncertainties on the measurement, and the following confidence intervals are measured at 95% CL:

$$\begin{aligned}|V_{tb}| &> 0.970 \\ |V_{td}|^2 + |V_{ts}|^2 &< 0.057.\end{aligned}\tag{8}$$

This measurement is comparable with the previous most precise estimate using $t\bar{t}$ events from Ref. [17], and with the result of the combination of single top quark measurements in Ref. [29].

8.2 Measurements for two BSM scenarios

Any BSM contribution potentially enhancing $|V_{tb}|^2$, $|V_{ts}|^2$, or $|V_{td}|^2$ can affect top quark production, decay, or both. Some BSM scenarios predict the presence of additional quark families. In this case, the CKM matrix is extended due to the mixing between the SM quarks and the new hypothesised ones. This would imply that the CKM matrix elements $|V_{tb}|$, $|V_{ts}|$, and $|V_{td}|$ would not necessarily satisfy the unitarity constraint of $|V_{tb}|^2 + |V_{ts}|^2 + |V_{td}|^2 = 1$. If these BSM quarks are heavier than the top quark, they would alter the CKM matrix elements without appearing as top quark decay products. They would thus not contribute directly to the top quark decay width Γ_t , but only indirectly because of the reduction in the absolute values of the corresponding SM CKM matrix elements.

For the first BSM scenario, we assume the top quark decays through the same channels as in the SM case, and that the partial width of each decay only varies because of a modified CKM matrix element. In this case, by writing Γ_t and $\tilde{\Gamma}_q$ as a function of $|V_{tb}|^2$ and $|V_{td}|^2 + |V_{ts}|^2$, Eq. (5) becomes:

$$\begin{aligned}\mu_b &= \frac{|V_{tb}|_{\text{obs}}^4}{|V_{tb}|^4 (|V_{tb}|_{\text{obs}}^2 + |V_{ts}|_{\text{obs}}^2 + |V_{td}|_{\text{obs}}^2)} \\ \mu_{\text{sd}} &= \frac{|V_{tb}|_{\text{obs}}^2 (|V_{ts}|_{\text{obs}}^2 + |V_{td}|_{\text{obs}}^2)}{(|V_{ts}|^2 + |V_{td}|^2) (|V_{tb}|_{\text{obs}}^2 + |V_{ts}|_{\text{obs}}^2 + |V_{td}|_{\text{obs}}^2)}.\end{aligned}\tag{9}$$

In this scenario, the measurement is performed leaving $|V_{tb}|$ and $|V_{td}|^2 + |V_{ts}|^2$ as free parameters in the fit, resulting in:

$$\begin{aligned}|V_{tb}| &= 0.988 \pm 0.027 \text{ (stat+prof)} \pm 0.043 \text{ (nonprof)} \\ |V_{td}|^2 + |V_{ts}|^2 &= 0.06 \pm 0.05 \text{ (stat+prof)} \begin{matrix} +0.04 \\ -0.03 \end{matrix} \text{ (nonprof)}.\end{aligned}\tag{10}$$

In the second BSM scenario, the top quark partial width is unchanged, but the total width increases due to additional, undetected decays. In the fit, the partial widths for decays to

known quarks are fixed, and the total width is a free parameter and allowed to vary. The effects on Γ_t due to variations in $|V_{tb}|^2$, $|V_{td}|^2$, and $|V_{ts}|^2$ are neglected.

In this scenario, Eq. (5) is modified to:

$$\begin{aligned}\mu_b &= \frac{|V_{tb}|_{\text{obs}}^4 \Gamma_t}{|V_{tb}|^4 \Gamma_t^{\text{obs}}} \\ \mu_{\text{sd}} &= \frac{|V_{tb}|_{\text{obs}}^2 (|V_{ts}|_{\text{obs}}^2 + |V_{td}|_{\text{obs}}^2) \Gamma_t}{|V_{tb}|^2 (|V_{ts}|^2 + |V_{td}|^2) \Gamma_t^{\text{obs}}}.\end{aligned}\tag{11}$$

Using $|V_{tb}|^2$, $|V_{td}|^2 + |V_{ts}|^2$, and $R_\Gamma = \Gamma_t^{\text{obs}}/\Gamma_t$ as the free parameters in the fit, we obtain:

$$\begin{aligned}|V_{tb}| &= 0.988 \pm 0.011 \text{ (stat+prof)} \pm 0.021 \text{ (nonprof)} \\ |V_{td}|^2 + |V_{ts}|^2 &= 0.06 \pm 0.05 \text{ (stat+prof)} \pm 0.04 \text{ (nonprof)} \\ R_\Gamma &= 0.99 \pm 0.42 \text{ (stat+prof)} \pm 0.03 \text{ (nonprof)}.\end{aligned}\tag{12}$$

The measured correlation factors between the three parameters are $\rho_{|V_{tb}|, |V_{td}|^2} = -0.19$, $\rho_{|V_{tb}|, R_\Gamma} = -0.78$, and $\rho_{R_\Gamma, |V_{td}|^2} = -0.21$. This measurement is in good agreement with the other measurements from Refs. [17, 29, 69, 70], which however make use of the SM assumptions. The results for the second BSM scenario have a higher statistical precision than those for the first scenario because of the weaker dependence of the signal strength on $|V_{tb}|$ for the first scenario.

As mentioned in Section 1, constraints on $|V_{td}|$ and $|V_{ts}|$ from precision low-energy measurements do not necessarily hold when BSM particles are present in the relevant Feynman diagram loops. Theoretical studies have shown that values of $|V_{ts}|$ up to about 0.2 are possible in some BSM scenarios [13]. The measurements presented here establish a model-independent upper limit on $|V_{td}|$ and $|V_{ts}|$ by removing any assumed theoretical hypotheses. This will now allow new interpretations for possible mixing of SM and BSM processes.

Alternative approaches interpret the available single top quark measurements in terms of different scenarios for modifying the CKM matrix elements (see, for example, Ref. [32]), obtaining results that are comparable with the measurements presented in this Letter. Such approaches, however, do not allow changes in the decay vertex of the top quark, and do not consider possible similarities in the features of the $ST_{b,q}$ signal and background processes.

The current analysis improves the precision on $|V_{tb}|$ by 50% with respect to previous studies [10] by exploiting the tWb vertex in the top quark decay, and is more precise than the combined ATLAS and CMS measurement using data at $\sqrt{s} = 7$ and 8 TeV [29].

9 Summary

A measurement of the Cabibbo–Kobayashi–Maskawa (CKM) matrix elements $|V_{tb}|$, $|V_{td}|$, and $|V_{ts}|$ has been performed in an event sample enriched in t -channel single top quark events, featuring one muon or electron and jets in the final state. The data are from proton-proton collisions at $\sqrt{s} = 13$ TeV, acquired at the LHC by the CMS experiment and correspond to an integrated luminosity of 35.9 fb^{-1} . The contributions from single top quark processes featuring all three matrix elements in the production vertex have been considered as separate signal processes, as well as contributions from decays of single top quarks involving all three quark families. The yields of the signal processes have been extracted through a simultaneous

fit to data in different selected event categories, and the values of the CKM matrix elements have been inferred from the signal strengths, which are the ratios of the measured top quark t -channel cross sections times branching ratios to the expected values. The signal strengths obtained from the fit are $\mu_b = 0.99 \pm 0.12$, where the uncertainty includes both the statistical and systematic components, and $\mu_{sd} < 87$ at 95% confidence level (CL).

Under the standard model assumption of CKM unitarity, the values are found to be $|V_{tb}| > 0.970$ and $|V_{td}|^2 + |V_{ts}|^2 < 0.057$, both at 95% CL.

Fits were also performed under two different beyond-the-standard-model scenarios. In the first, we assume the presence of additional quark families that are heavier than the top quark. The unitarity constraint for the three CKM matrix elements no longer holds, but the top quark decays through the same channels as in the standard model. We assume the partial width of each top quark decay only varies because of a modified CKM matrix element. The fit gives:

$$\begin{aligned} |V_{tb}| &= 0.988 \pm 0.051 \\ |V_{td}|^2 + |V_{ts}|^2 &= 0.06 \pm 0.06, \end{aligned}$$

where the uncertainties include both the statistical and systematic components.

In the second scenario, the top quark width is left unconstrained under the assumption that the contributions to the total width from the mixing of the three families are negligible. The corresponding measured values are:

$$\begin{aligned} |V_{tb}| &= 0.988 \pm 0.024, \\ |V_{td}|^2 + |V_{ts}|^2 &= 0.06 \pm 0.06, \\ \frac{\Gamma_t^{\text{obs}}}{\Gamma_t} &= 0.99 \pm 0.42, \end{aligned}$$

where again, both the statistical and systematic uncertainties are included. The differences among the uncertainties in the presented scenarios are driven by the difference in the functional dependence of the observed event yields from the CKM matrix elements. This results in smaller uncertainties in $|V_{tb}|$ for the case where a fourth-power dependence is considered with respect to the second-power dependence case.

All results are consistent with each other, and show no deviation with respect to extrapolations of low-energy measurements. These results are the first direct, model-independent measurements of the CKM matrix elements for the third-generation quarks, and provide the best determination of these fundamental SM parameters via single top quark measurements.

Acknowledgments

We congratulate our colleagues in the CERN accelerator departments for the excellent performance of the LHC and thank the technical and administrative staffs at CERN and at other CMS institutes for their contributions to the success of the CMS effort. In addition, we gratefully acknowledge the computing centres and personnel of the Worldwide LHC Computing Grid for delivering so effectively the computing infrastructure essential to our analyses. Finally, we acknowledge the enduring support for the construction and operation of the LHC and the CMS detector provided by the following funding agencies: BMBWF and FWF (Austria); FNRS and FWO (Belgium); CNPq, CAPES, FAPERJ, FAPERGS, and FAPESP (Brazil); MES (Bulgaria); CERN; CAS, MoST, and NSFC (China); COLCIENCIAS (Colombia); MSES and CSF (Croatia);

RPF (Cyprus); SENESCYT (Ecuador); MoER, ERC IUT, PUT and ERDF (Estonia); Academy of Finland, MEC, and HIP (Finland); CEA and CNRS/IN2P3 (France); BMBF, DFG, and HGF (Germany); GSRT (Greece); NKFIA (Hungary); DAE and DST (India); IPM (Iran); SFI (Ireland); INFN (Italy); MSIP and NRF (Republic of Korea); MES (Latvia); LAS (Lithuania); MOE and UM (Malaysia); BUAP, CINVESTAV, CONACYT, LNS, SEP, and UASLP-FAI (Mexico); MOS (Montenegro); MBIE (New Zealand); PAEC (Pakistan); MSHE and NSC (Poland); FCT (Portugal); JINR (Dubna); MON, RosAtom, RAS, RFBR, and NRC KI (Russia); MESTD (Serbia); SEIDI, CPAN, PCTI, and FEDER (Spain); MOSTR (Sri Lanka); Swiss Funding Agencies (Switzerland); MST (Taipei); ThEPCenter, IPST, STAR, and NSTDA (Thailand); TUBITAK and TAEK (Turkey); NASU (Ukraine); STFC (United Kingdom); DOE and NSF (USA).

Individuals have received support from the Marie-Curie programme and the European Research Council and Horizon 2020 Grant, contract Nos. 675440, 752730, and 765710 (European Union); the Leventis Foundation; the A.P. Sloan Foundation; the Alexander von Humboldt Foundation; the Belgian Federal Science Policy Office; the Fonds pour la Formation à la Recherche dans l'Industrie et dans l'Agriculture (FRIA-Belgium); the Agentschap voor Innovatie door Wetenschap en Technologie (IWT-Belgium); the F.R.S.-FNRS and FWO (Belgium) under the "Excellence of Science – EOS" – be.h project n. 30820817; the Beijing Municipal Science & Technology Commission, No. Z191100007219010; the Ministry of Education, Youth and Sports (MEYS) of the Czech Republic; the Deutsche Forschungsgemeinschaft (DFG) under Germany's Excellence Strategy – EXC 2121 "Quantum Universe" – 390833306; the Lendület ("Momentum") Programme and the János Bolyai Research Scholarship of the Hungarian Academy of Sciences, the New National Excellence Program ÚNKP, the NKFIA research grants 123842, 123959, 124845, 124850, 125105, 128713, 128786, and 129058 (Hungary); the Council of Science and Industrial Research, India; the HOMING PLUS programme of the Foundation for Polish Science, cofinanced from European Union, Regional Development Fund, the Mobility Plus programme of the Ministry of Science and Higher Education, the National Science Center (Poland), contracts Harmonia 2014/14/M/ST2/00428, Opus 2014/13/B/ST2/02543, 2014/15/B/ST2/03998, and 2015/19/B/ST2/02861, Sonata-bis 2012/07/E/ST2/01406; the National Priorities Research Program by Qatar National Research Fund; the Ministry of Science and Education, grant no. 14.W03.31.0026 (Russia); the Tomsk Polytechnic University Competitiveness Enhancement Program and "Nauka" Project FSWW-2020-0008 (Russia); the Programa Estatal de Fomento de la Investigación Científica y Técnica de Excelencia María de Maeztu, grant MDM-2015-0509 and the Programa Severo Ochoa del Principado de Asturias; the Thalís and Aristeia programmes cofinanced by EU-ESF and the Greek NSRF; the Rachadapisek Sompot Fund for Postdoctoral Fellowship, Chulalongkorn University and the Chulalongkorn Academic into Its 2nd Century Project Advancement Project (Thailand); the Kavli Foundation; the Nvidia Corporation; the SuperMicro Corporation; the Welch Foundation, contract C-1845; and the Weston Havens Foundation (USA).

References

- [1] M. Kobayashi and T. Maskawa, "CP-violation in the renormalizable theory of weak interaction", *Prog. Theor. Phys.* **49** (1973) 652, doi:10.1143/PTP.49.652.
- [2] CMS Collaboration, "Measurement of the t -channel single top quark production cross section in pp collisions at $\sqrt{s} = 7$ TeV", *Phys. Rev. Lett.* **107** (2011) 091802, doi:10.1103/PhysRevLett.107.091802, arXiv:1106.3052.

- [3] CMS Collaboration, “Measurement of the single-top-quark t -channel cross section in pp collisions at $\sqrt{s} = 7$ TeV”, *JHEP* **12** (2012) 035, doi:10.1007/JHEP12(2012)035, arXiv:1209.4533.
- [4] ATLAS Collaboration, “Measurement of the t -channel single top-quark production cross section in pp collisions at $\sqrt{s} = 7$ TeV with the ATLAS detector”, *Phys. Lett. B* **717** (2012) 330, doi:10.1016/j.physletb.2012.09.031, arXiv:1205.3130.
- [5] ATLAS Collaboration, “Comprehensive measurements of t -channel single top-quark production cross sections at $\sqrt{s} = 7$ TeV with the ATLAS detector”, *Phys. Rev. D* **90** (2014) 112006, doi:10.1103/PhysRevD.90.112006, arXiv:1406.7844.
- [6] CMS Collaboration, “Measurement of the t -channel single-top-quark production cross section and of the $|V_{tb}|$ CKM matrix element in pp collisions at $\sqrt{s} = 8$ TeV”, *JHEP* **06** (2014) 090, doi:10.1007/JHEP06(2014)090, arXiv:1403.7366.
- [7] ATLAS Collaboration, “Measurement of the inclusive cross-sections of single top-quark and top-antiquark t -channel production in pp collisions at $\sqrt{s} = 13$ TeV with the ATLAS detector”, *JHEP* **04** (2017) 086, doi:10.1007/JHEP04(2017)086, arXiv:1609.03920.
- [8] CMS Collaboration, “Cross section measurement of t -channel single top quark production in pp collisions at $\sqrt{s} = 13$ TeV”, *Phys. Lett. B* **772** (2017) 752, doi:10.1016/j.physletb.2017.07.047, arXiv:1610.00678.
- [9] ATLAS Collaboration, “Fiducial, total and differential cross-section measurements of t -channel single top-quark production in pp collisions at 8 TeV using data collected by the ATLAS detector”, *Eur. Phys. J. C* **77** (2017) 531, doi:10.1140/epjc/s10052-017-5061-9, arXiv:1702.02859.
- [10] CMS Collaboration, “Measurement of the single top quark and antiquark production cross sections in the t channel and their ratio in proton-proton collisions at $\sqrt{s} = 13$ TeV”, *Phys. Lett. B* **800** (2019) 135042, doi:10.1016/j.physletb.2019.135042, arXiv:1812.10514.
- [11] CMS Collaboration, “Measurement of differential cross sections and charge ratios for t -channel single top quark production in proton-proton collisions at $\sqrt{s} = 13$ TeV”, *Eur. Phys. J. C* **80** (2020), no. 5, 370, doi:10.1140/epjc/s10052-020-7858-1, arXiv:1907.08330.
- [12] Particle Data Group, M. Tanabashi et al., “Review of particle physics”, *Phys. Rev. D* **98** (2018) 030001, doi:10.1103/PhysRevD.98.030001.
- [13] J. Alwall et al., “Is $V_{tb} \simeq 1$?”, *Eur. Phys. J. C* **49** (2007) 791, doi:10.1140/epjc/s10052-006-0137-y, arXiv:hep-ph/0607115.
- [14] D0 Collaboration, “Precision measurement of the ratio $\mathcal{B}(t \rightarrow Wb)/\mathcal{B}(t \rightarrow Wq)$ and extraction of V_{tb} ”, *Phys. Rev. Lett.* **107** (2011) 121802, doi:10.1103/PhysRevLett.107.121802, arXiv:1106.5436.
- [15] CDF Collaboration, “Measurement of $R = \mathcal{B}(t \rightarrow Wb)/\mathcal{B}(t \rightarrow Wq)$ in top-quark-pair decays using lepton+jets events and the full CDF Run II data set”, *Phys. Rev. D* **87** (2013) 111101, doi:10.1103/PhysRevD.87.111101, arXiv:1303.6142.

-
- [16] CDF Collaboration, “Measurement of $\mathcal{B}(t \rightarrow Wb)/\mathcal{B}(t \rightarrow Wq)$ in top-quark-pair decays using dilepton events and the full CDF Run II data set”, *Phys. Rev. Lett.* **112** (2014) 221801, doi:10.1103/PhysRevLett.112.221801, arXiv:1404.3392.
- [17] CMS Collaboration, “Measurement of the ratio $\mathcal{B}(t \rightarrow Wb)/\mathcal{B}(t \rightarrow Wq)$ in pp collisions at $\sqrt{s} = 8$ TeV”, *Phys. Lett. B* **736** (2014) 33, doi:10.1016/j.physletb.2014.06.076, arXiv:1404.2292.
- [18] D0 Collaboration, “Evidence for production of single top quarks and first direct measurement of $|V_{tb}|$ ”, *Phys. Rev. Lett.* **98** (2007) 181802, doi:10.1103/PhysRevLett.98.181802, arXiv:hep-ex/0612052.
- [19] D0 Collaboration, “Evidence for production of single top quarks”, *Phys. Rev. D* **78** (2008) 012005, doi:10.1103/PhysRevD.78.012005, arXiv:0803.0739.
- [20] CDF Collaboration, “Measurement of the single-top-quark production cross section at CDF”, *Phys. Rev. Lett.* **101** (2008) 252001, doi:10.1103/PhysRevLett.101.252001, arXiv:0809.2581.
- [21] CDF Collaboration, “Observation of electroweak single top quark production”, *Phys. Rev. Lett.* **103** (2009) 092002, doi:10.1103/PhysRevLett.103.092002, arXiv:0903.0885.
- [22] CDF Collaboration, “Observation of single top quark production and measurement of $|V_{tb}|$ with CDF”, *Phys. Rev. D* **82** (2010) 112005, doi:10.1103/PhysRevD.82.112005, arXiv:1004.1181.
- [23] D0 Collaboration, “Observation of single top-quark production”, *Phys. Rev. Lett.* **103** (2009) 092001, doi:10.1103/PhysRevLett.103.092001, arXiv:0903.0850.
- [24] The CDF Collaboration, The D0 Collaboration, The Tevatron electroweak working group, “Combination of CDF and D0 measurements of the single top production cross section”, (2009). arXiv:0908.2171.
- [25] CDF Collaboration, “Measurement of the single top quark production cross section and $|V_{tb}|$ in events with one charged lepton, large missing transverse energy, and jets at CDF”, *Phys. Rev. Lett.* **113** (2014) 261804, doi:10.1103/PhysRevLett.113.261804, arXiv:1407.4031.
- [26] D0 Collaboration, “Evidence for s-channel single top quark production in $p\bar{p}$ collisions at $\sqrt{s} = 1.96$ TeV”, *Phys. Lett. B* **726** (2013) 656, doi:10.1016/j.physletb.2013.09.048, arXiv:1307.0731.
- [27] CDF, D0 Collaboration, “Observation of s-channel production of single top quarks at the Tevatron”, *Phys. Rev. Lett.* **112** (2014) 231803, doi:10.1103/PhysRevLett.112.231803, arXiv:1402.5126.
- [28] CMS Collaboration, “Search for anomalous Wtb couplings and flavour-changing neutral currents in t-channel single top quark production in pp collisions at $\sqrt{s} = 7$ and 8 TeV”, *JHEP* **02** (2017) 028, doi:10.1007/JHEP02(2017)028, arXiv:1610.03545.
- [29] ATLAS, CMS Collaboration, “Combinations of single-top-quark production cross-section measurements and $|f_{LV}V_{tb}|$ determinations at $\sqrt{s} = 7$ and 8 TeV with the ATLAS and CMS experiments”, *JHEP* **05** (2019) 088, doi:10.1007/JHEP05(2019)088, arXiv:1902.07158.

- [30] H. Lacker et al., “Model-independent extraction of $|V_{tq}|$ matrix elements from top-quark measurements at hadron colliders”, *Eur. Phys. J. C* **72** (2012) 2048, doi:10.1140/epjc/s10052-012-2048-4, arXiv:1202.4694.
- [31] J. A. Aguilar-Saavedra and A. Onofre, “Using single top rapidity to measure V_{td} , V_{ts} , V_{tb} at hadron colliders”, *Phys. Rev. D* **83** (2011) 073003, doi:10.1103/PhysRevD.83.073003, arXiv:1002.4718.
- [32] B. Clerbaux, W. Fang, A. Giammanco, and R. Goldouzian, “Model-independent constraints on the CKM matrix elements $|V_{tb}|$, $|V_{ts}|$ and $|V_{td}|$ ”, *JHEP* **03** (2019) 022, doi:10.1007/JHEP03(2019)022, arXiv:1807.07319.
- [33] E. Alvarez, L. Da Rold, M. Estevez, and J. F. Kamenik, “Measuring $|V_{td}|$ at the LHC”, *Phys. Rev. D* **97** (2018) 033002, doi:10.1103/PhysRevD.97.033002, arXiv:1709.07887.
- [34] A. Giammanco and R. Schwienhorst, “Single top-quark production at the Tevatron and the LHC”, *Rev. Mod. Phys.* **90** (2018) 035001, doi:10.1103/RevModPhys.90.035001, arXiv:1710.10699.
- [35] CMS Collaboration, “The CMS experiment at the CERN LHC”, *JINST* **3** (2008) S08004, doi:10.1088/1748-0221/3/08/S08004.
- [36] CMS Collaboration, “The CMS trigger system”, *JINST* **12** (2017) P01020, doi:10.1088/1748-0221/12/01/P01020, arXiv:1609.02366.
- [37] P. Nason, “A new method for combining NLO QCD with shower Monte Carlo algorithms”, *JHEP* **11** (2004) 040, doi:10.1088/1126-6708/2004/11/040, arXiv:hep-ph/0409146.
- [38] S. Frixione, P. Nason, and C. Oleari, “Matching NLO QCD computations with parton shower simulations: the POWHEG method”, *JHEP* **11** (2007) 070, doi:10.1088/1126-6708/2007/11/070, arXiv:0709.2092.
- [39] S. Alioli, P. Nason, C. Oleari, and E. Re, “A general framework for implementing NLO calculations in shower Monte Carlo programs: the POWHEG BOX”, *JHEP* **06** (2010) 043, doi:10.1007/JHEP06(2010)043, arXiv:1002.2581.
- [40] R. Frederix, E. Re, and P. Torrielli, “Single-top t -channel hadroproduction in the four-flavour scheme with POWHEG and aMC@NLO”, *JHEP* **09** (2012) 130, doi:10.1007/JHEP09(2012)130, arXiv:1207.5391.
- [41] S. Alioli, P. Nason, C. Oleari, and E. Re, “NLO single-top production matched with shower in POWHEG: s - and t -channel contributions”, *JHEP* **09** (2009) 111, doi:10.1088/1126-6708/2009/09/111, arXiv:0907.4076.
- [42] P. Artoisenet, R. Frederix, O. Mattelaer, and R. Rietkerk, “Automatic spin-entangled decays of heavy resonances in Monte Carlo simulations”, *JHEP* **03** (2013) 015, doi:10.1007/JHEP03(2013)015, arXiv:1212.3460.
- [43] S. Frixione, P. Nason, and G. Ridolfi, “A positive-weight next-to-leading-order Monte Carlo for heavy flavour hadroproduction”, *JHEP* **09** (2007) 126, doi:10.1088/1126-6708/2007/09/126, arXiv:0707.3088.

-
- [44] T. Melia, P. Nason, R. Rötsch, and G. Zanderighi, “ W^+W^- , WZ and ZZ production in the POWHEG BOX”, *JHEP* **11** (2011) 078, doi:10.1007/JHEP11(2011)078, arXiv:1107.5051.
- [45] P. Nason and G. Zanderighi, “ W^+W^- , WZ and ZZ production in the POWHEG-BOX-V2”, *Eur. Phys. J. C* **74** (2014) 2702, doi:10.1140/epjc/s10052-013-2702-5, arXiv:1311.1365.
- [46] E. Re, “Single-top Wt -channel production matched with parton showers using the POWHEG method”, *Eur. Phys. J. C* **71** (2011) 1547, doi:10.1140/epjc/s10052-011-1547-z, arXiv:1009.2450.
- [47] J. Alwall et al., “The automated computation of tree-level and next-to-leading order differential cross sections, and their matching to parton shower simulations”, *JHEP* **07** (2014) 079, doi:10.1007/JHEP07(2014)079, arXiv:1405.0301.
- [48] T. Sjöstrand, S. Mrenna, and P. Z. Skands, “A brief introduction to PYTHIA 8.1”, *Comput. Phys. Commun.* **178** (2008) 852, doi:10.1016/j.cpc.2008.01.036, arXiv:0710.3820.
- [49] CMS Collaboration, “Event generator tunes obtained from underlying event and multiparton scattering measurements”, *Eur. Phys. J. C* **76** (2016) 155, doi:10.1140/epjc/s10052-016-3988-x, arXiv:1512.00815.
- [50] CMS Collaboration, “Investigations of the impact of the parton shower tuning in PYTHIA 8 in the modelling of $t\bar{t}$ at $\sqrt{s} = 8$ and 13 TeV”, CMS Physics Analysis Summary CMS-PAS-TOP-16-021, 2016.
- [51] R. Frederix and S. Frixione, “Merging meets matching in MC@NLO”, *JHEP* **12** (2012) 061, doi:10.1007/JHEP12(2012)061, arXiv:1209.6215.
- [52] NNPDF Collaboration, “Parton distributions for the LHC Run II”, *JHEP* **04** (2015) 040, doi:10.1007/JHEP04(2015)040, arXiv:1410.8849.
- [53] GEANT4 Collaboration, “GEANT4—a simulation toolkit”, *Nucl. Instrum. Meth. A* **506** (2003) 250, doi:10.1016/S0168-9002(03)01368-8.
- [54] M. Cacciari, G. P. Salam, and G. Soyez, “Fastjet user manual”, *Eur. Phys. J. C* **72** (2012) 1896, doi:10.1140/epjc/s10052-012-1896-2, arXiv:1111.6097.
- [55] M. Cacciari, G. P. Salam, and G. Soyez, “The anti- k_T jet clustering algorithm”, *JHEP* **04** (2008) 063, doi:10.1088/1126-6708/2008/04/063, arXiv:0802.1189.
- [56] CMS Collaboration, “Particle-flow reconstruction and global event description with the CMS detector”, *JINST* **12** (2017) P10003, doi:10.1088/1748-0221/12/10/P10003, arXiv:1706.04965.
- [57] CMS Collaboration, “Performance of the CMS muon detector and muon reconstruction with proton-proton collisions at $\sqrt{s} = 13$ TeV”, *JINST* **13** (2018) P06015, doi:10.1088/1748-0221/13/06/P06015, arXiv:1804.04528.
- [58] M. Cacciari and G. P. Salam, “Pileup subtraction using jet areas”, *Phys. Lett. B* **659** (2008) 119, doi:10.1016/j.physletb.2007.09.077, arXiv:0707.1378.

- [59] CMS Collaboration, “Jet energy scale and resolution in the CMS experiment in pp collisions at 8 TeV”, *JINST* **12** (2017) P02014, doi:10.1088/1748-0221/12/02/P02014, arXiv:1607.03663.
- [60] CMS Collaboration, “Identification of b-quark jets with the CMS experiment”, *JINST* **8** (2013) P04013, doi:10.1088/1748-0221/8/04/P04013, arXiv:1211.4462.
- [61] CMS Collaboration, “Identification of heavy-flavour jets with the CMS detector in pp collisions at 13 TeV”, *JINST* **13** (2018) P05011, doi:10.1088/1748-0221/13/05/P05011, arXiv:1712.07158.
- [62] M. Aliev et al., “HATHOR – HAdronic Top and Heavy quarks crOss section calculatoR”, *Comput. Phys. Commun.* **182** (2011) 1034, doi:10.1016/j.cpc.2010.12.040, arXiv:1007.1327.
- [63] R. Barlow and C. Beeston, “Fitting using finite Monte Carlo samples”, *Comput. Phys. Commun.* **77** (1993) 219, doi:10.1016/0010-4655(93)90005-W.
- [64] J. S. Conway, “Nuisance parameters in likelihoods for multisource spectra”, in *Proceedings of PHYSTAT 2011 Workshop on Statistical Issues Related to Discovery Claims in Search Experiments and Unfolding*, H. Prosper and L. Lyons, eds., number CERN-2011-006, p. 115. CERN, 2011.
- [65] CMS Collaboration, “Measurements of inclusive W and Z cross sections in pp collisions at $\sqrt{s} = 7$ TeV”, *JHEP* **01** (2011) 080, doi:10.1007/JHEP01(2011)080, arXiv:1012.2466.
- [66] CMS Collaboration, “Measurement of the inelastic proton-proton cross section at $\sqrt{s} = 13$ TeV”, *JHEP* **07** (2018) 161, doi:10.1007/JHEP07(2018)161, arXiv:1802.02613.
- [67] J. Butterworth et al., “PDF4LHC recommendations for LHC run II”, *J. Phys. G* **43** (2016) 023001, doi:10.1088/0954-3899/43/2/023001, arXiv:1510.03865.
- [68] CMS Collaboration, “CMS luminosity measurements for the 2016 data taking period”, CMS Physics Analysis Summary CMS-PAS-LUM-17-001, 2017.
- [69] D0 Collaboration, “Improved determination of the width of the top quark”, *Phys. Rev. D* **85** (2012) 091104, doi:10.1103/PhysRevD.85.091104, arXiv:1201.4156.
- [70] ATLAS Collaboration, “Direct top-quark decay width measurement in the $t\bar{t}$ lepton+jets channel at $\sqrt{s} = 8$ TeV with the ATLAS experiment”, *Eur. Phys. J. C* **78** (2018) 129, doi:10.1140/epjc/s10052-018-5595-5, arXiv:1709.04207.

A The CMS Collaboration

Yerevan Physics Institute, Yerevan, Armenia

A.M. Sirunyan[†], A. Tumasyan

Institut für Hochenergiephysik, Wien, Austria

W. Adam, F. Ambrogi, T. Bergauer, M. Dragicevic, J. Erö, A. Escalante Del Valle, M. Flechl, R. Frühwirth¹, M. Jeitler¹, N. Krammer, I. Krätschmer, D. Liko, T. Madlener, I. Mikulec, N. Rad, J. Schieck¹, R. Schöfbeck, M. Spanring, W. Waltenberger, C.-E. Wulz¹, M. Zarucki

Institute for Nuclear Problems, Minsk, Belarus

V. Drugakov, V. Mossolov, J. Suarez Gonzalez

Universiteit Antwerpen, Antwerpen, Belgium

M.R. Darwish, E.A. De Wolf, D. Di Croce, X. Janssen, T. Kello², A. Lelek, M. Pieters, H. Rejeb Sfar, H. Van Haevermaet, P. Van Mechelen, S. Van Putte, N. Van Remortel

Vrije Universiteit Brussel, Brussel, Belgium

F. Blekman, E.S. Bols, S.S. Chhibra, J. D'Hondt, J. De Clercq, D. Lontkovskyi, S. Lowette, I. Marchesini, S. Moortgat, Q. Python, S. Tavernier, W. Van Doninck, P. Van Mulders

Université Libre de Bruxelles, Bruxelles, Belgium

D. Beghin, B. Bilin, B. Clerbaux, G. De Lentdecker, H. Delannoy, B. Dorney, L. Favart, A. Grebenyuk, A.K. Kalsi, L. Moureaux, A. Popov, N. Postiau, E. Starling, L. Thomas, C. Vander Velde, P. Vanlaer, D. Vannerom

Ghent University, Ghent, Belgium

T. Cornelis, D. Dobur, I. Khvastunov³, M. Niedziela, C. Roskas, K. Skovpen, M. Tytgat, W. Verbeke, B. Vermassen, M. Vit

Université Catholique de Louvain, Louvain-la-Neuve, Belgium

G. Bruno, C. Caputo, P. David, C. Delaere, M. Delcourt, A. Giammanco, V. Lemaitre, J. Prisciandaro, A. Saggio, P. Vischia, J. Zobec

Centro Brasileiro de Pesquisas Físicas, Rio de Janeiro, Brazil

G.A. Alves, G. Correia Silva, C. Hensel, A. Moraes

Universidade do Estado do Rio de Janeiro, Rio de Janeiro, Brazil

E. Belchior Batista Das Chagas, W. Carvalho, J. Chinellato⁴, E. Coelho, E.M. Da Costa, G.G. Da Silveira⁵, D. De Jesus Damiao, C. De Oliveira Martins, S. Fonseca De Souza, H. Malbouisson, J. Martins⁶, D. Matos Figueiredo, M. Medina Jaime⁷, M. Melo De Almeida, C. Mora Herrera, L. Mundim, H. Nogima, W.L. Prado Da Silva, P. Rebello Teles, L.J. Sanchez Rosas, A. Santoro, A. Sznajder, M. Thiel, E.J. Tonelli Manganote⁴, F. Torres Da Silva De Araujo, A. Vilela Pereira

Universidade Estadual Paulista ^a, Universidade Federal do ABC ^b, São Paulo, Brazil

C.A. Bernardes^a, L. Calligaris^a, T.R. Fernandez Perez Tomei^a, E.M. Gregores^b, D.S. Lemos, P.G. Mercadante^b, S.F. Novaes^a, Sandra S. Padula^a

Institute for Nuclear Research and Nuclear Energy, Bulgarian Academy of Sciences, Sofia, Bulgaria

A. Aleksandrov, G. Antchev, R. Hadjiiska, P. Iaydjiev, M. Misheva, M. Rodozov, M. Shopova, G. Sultanov

University of Sofia, Sofia, Bulgaria

M. Bonchev, A. Dimitrov, T. Ivanov, L. Litov, B. Pavlov, P. Petkov, A. Petrov

Beihang University, Beijing, ChinaW. Fang², X. Gao², L. Yuan**Department of Physics, Tsinghua University, Beijing, China**

M. Ahmad, Z. Hu, Y. Wang

Institute of High Energy Physics, Beijing, ChinaG.M. Chen⁸, H.S. Chen⁸, M. Chen, C.H. Jiang, D. Leggat, H. Liao, Z. Liu, A. Spiezia, J. Tao, E. Yazgan, H. Zhang, S. Zhang⁸, J. Zhao**State Key Laboratory of Nuclear Physics and Technology, Peking University, Beijing, China**

A. Agapitos, Y. Ban, G. Chen, A. Levin, J. Li, L. Li, Q. Li, Y. Mao, S.J. Qian, D. Wang, Q. Wang

Zhejiang University, Hangzhou, China

M. Xiao

Universidad de Los Andes, Bogota, Colombia

C. Avila, A. Cabrera, C. Florez, C.F. González Hernández, M.A. Segura Delgado

Universidad de Antioquia, Medellin, Colombia

J. Mejia Guisao, J.D. Ruiz Alvarez, C.A. Salazar González, N. Vanegas Arbelaez

University of Split, Faculty of Electrical Engineering, Mechanical Engineering and Naval Architecture, Split, Croatia

D. Giljanović, N. Godinovic, D. Lelas, I. Puljak, T. Sculac

University of Split, Faculty of Science, Split, Croatia

Z. Antunovic, M. Kovac

Institute Rudjer Boskovic, Zagreb, CroatiaV. Brigljevic, D. Ferencek, K. Kadija, B. Mesic, M. Roguljic, A. Starodumov⁹, T. Susa**University of Cyprus, Nicosia, Cyprus**

M.W. Ather, A. Attikis, E. Erodotou, A. Ioannou, M. Kolosova, S. Konstantinou, G. Mavromanolakis, J. Mousa, C. Nicolaou, F. Ptochos, P.A. Razis, H. Rykaczewski, H. Saka, D. Tsiakkouri

Charles University, Prague, Czech RepublicM. Finger¹⁰, M. Finger Jr.¹⁰, A. Kveton, J. Tomsa**Escuela Politecnica Nacional, Quito, Ecuador**

E. Ayala

Universidad San Francisco de Quito, Quito, Ecuador

E. Carrera Jarrin

Academy of Scientific Research and Technology of the Arab Republic of Egypt, Egyptian Network of High Energy Physics, Cairo, EgyptA.A. Abdelalim^{11,12}, S. Abu Zeid**National Institute of Chemical Physics and Biophysics, Tallinn, Estonia**

S. Bhowmik, A. Carvalho Antunes De Oliveira, R.K. Dewanjee, K. Ehataht, M. Kadastik, M. Raidal, C. Veelken

Department of Physics, University of Helsinki, Helsinki, Finland

P. Eerola, L. Forthomme, H. Kirschenmann, K. Osterberg, M. Voutilainen

Helsinki Institute of Physics, Helsinki, Finland

F. Garcia, J. Havukainen, J.K. Heikkilä, V. Karimäki, M.S. Kim, R. Kinnunen, T. Lampén, K. Lassila-Perini, S. Laurila, S. Lehti, T. Lindén, H. Siikonen, E. Tuominen, J. Tuominiemi

Lappeenranta University of Technology, Lappeenranta, Finland

P. Luukka, T. Tuuva

IRFU, CEA, Université Paris-Saclay, Gif-sur-Yvette, France

M. Besancon, F. Couderc, M. Dejardin, D. Denegri, B. Fabbro, J.L. Faure, F. Ferri, S. Ganjour, A. Givernaud, P. Gras, G. Hamel de Monchenault, P. Jarry, C. Leloup, B. Lenzi, E. Locci, J. Malcles, J. Rander, A. Rosowsky, M.Ö. Sahin, A. Savoy-Navarro¹³, M. Titov, G.B. Yu

Laboratoire Leprince-Ringuet, CNRS/IN2P3, Ecole Polytechnique, Institut Polytechnique de Paris

S. Ahuja, C. Amendola, F. Beaudette, M. Bonanomi, P. Busson, C. Charlot, B. Diab, G. Falmagne, R. Granier de Cassagnac, I. Kucher, A. Lobanov, C. Martin Perez, M. Nguyen, C. Ochando, P. Paganini, J. Rembser, R. Salerno, J.B. Sauvan, Y. Sirois, A. Zabi, A. Zghiche

Université de Strasbourg, CNRS, IPHC UMR 7178, Strasbourg, France

J.-L. Agram¹⁴, J. Andrea, D. Bloch, G. Bourgatte, J.-M. Brom, E.C. Chabert, C. Collard, E. Conte¹⁴, J.-C. Fontaine¹⁴, D. Gelé, U. Goerlach, C. Grimault, A.-C. Le Bihan, N. Tonon, P. Van Hove

Centre de Calcul de l'Institut National de Physique Nucleaire et de Physique des Particules, CNRS/IN2P3, Villeurbanne, France

S. Gadrat

Université de Lyon, Université Claude Bernard Lyon 1, CNRS-IN2P3, Institut de Physique Nucléaire de Lyon, Villeurbanne, France

S. Beauceron, C. Bernet, G. Boudoul, C. Camen, A. Carle, N. Chanon, R. Chierici, D. Contardo, P. Depasse, H. El Mamouni, J. Fay, S. Gascon, M. Gouzevitch, B. Ille, Sa. Jain, I.B. Laktineh, H. Lattaud, A. Lesauvage, M. Lethuillier, L. Mirabito, S. Perries, V. Sordini, L. Torterotot, G. Touquet, M. Vander Donckt, S. Viret

Georgian Technical University, Tbilisi, Georgia

T. Toriashvili¹⁵

Tbilisi State University, Tbilisi, Georgia

Z. Tsamalaidze¹⁰

RWTH Aachen University, I. Physikalisches Institut, Aachen, Germany

C. Autermann, L. Feld, K. Klein, M. Lipinski, D. Meuser, A. Pauls, M. Preuten, M.P. Rauch, J. Schulz, M. Teroerde

RWTH Aachen University, III. Physikalisches Institut A, Aachen, Germany

M. Erdmann, B. Fischer, S. Ghosh, T. Hebbeker, K. Hoepfner, H. Keller, L. Mastrolorenzo, M. Merschmeyer, A. Meyer, P. Millet, G. Mocellin, S. Mondal, S. Mukherjee, D. Noll, A. Novak, T. Pook, A. Pozdnyakov, T. Quast, M. Radziej, Y. Rath, H. Reithler, J. Roemer, A. Schmidt, S.C. Schuler, A. Sharma, S. Wiedenbeck, S. Zaleski

RWTH Aachen University, III. Physikalisches Institut B, Aachen, Germany

G. Flügge, W. Haj Ahmad¹⁶, O. Hlushchenko, T. Kress, T. Müller, A. Nowack, C. Pistone, O. Pooth, D. Roy, H. Sert, A. Stahl¹⁷

Deutsches Elektronen-Synchrotron, Hamburg, Germany

M. Aldaya Martin, P. Asmuss, I. Babounikau, H. Bakhshiansohi, K. Beernaert, O. Behnke, A. Bermúdez Martínez, A.A. Bin Anuar, K. Borrás¹⁸, V. Botta, A. Campbell, A. Cardini, P. Connor, S. Consuegra Rodríguez, C. Contreras-Campana, V. Danilov, A. De Wit, M.M. Defranchis, C. Diez Pardos, D. Domínguez Damiani, G. Eckerlin, D. Eckstein, T. Eichhorn, A. Elwood, E. Eren, L.I. Estevez Banos, E. Gallo¹⁹, A. Geiser, A. Grohsjean, M. Guthoff, M. Haranko, A. Harb, A. Jafari, N.Z. Jomhari, H. Jung, A. Kasem¹⁸, M. Kasemann, H. Kaveh, J. Keaveney, C. Kleinwort, J. Knolle, D. Krücker, W. Lange, T. Lenz, J. Lidrych, K. Lipka, W. Lohmann²⁰, R. Mankel, I.-A. Melzer-Pellmann, A.B. Meyer, M. Meyer, M. Missiroli, J. Mnich, A. Mussgiller, V. Myronenko, D. Pérez Adán, S.K. Pflitsch, D. Pitzl, A. Raspereza, A. Saibel, M. Savitskyi, V. Scheurer, P. Schütze, C. Schwanenberger, R. Shevchenko, A. Singh, R.E. Sosa Ricardo, H. Tholen, O. Turkot, A. Vagnerini, M. Van De Klundert, R. Walsh, Y. Wen, K. Wichmann, C. Wissing, O. Zenaiev, R. Zlebcik

University of Hamburg, Hamburg, Germany

R. Aggleton, S. Bein, L. Benato, A. Benecke, T. Dreyer, A. Ebrahimi, F. Feindt, A. Fröhlich, C. Garbers, E. Garutti, D. Gonzalez, P. Gunnellini, J. Haller, A. Hinzmann, A. Karavdina, G. Kasieczka, R. Klanner, R. Kogler, N. Kovalchuk, S. Kurz, V. Kutzner, J. Lange, T. Lange, A. Malara, J. Multhaupt, C.E.N. Niemeyer, A. Reimers, O. Rieger, P. Schleper, S. Schumann, J. Schwandt, J. Sonneveld, H. Stadie, G. Steinbrück, B. Vormwald, I. Zoi

Karlsruher Institut fuer Technologie, Karlsruhe, Germany

M. Akbiyik, M. Baselga, S. Baur, T. Berger, E. Butz, R. Caspart, T. Chwalek, W. De Boer, A. Dierlamm, K. El Morabit, N. Faltermann, M. Giffels, A. Gottmann, F. Hartmann¹⁷, C. Heidecker, U. Husemann, M.A. Iqbal, S. Kudella, S. Maier, S. Mitra, M.U. Mozer, D. Müller, Th. Müller, M. Musich, A. Nürnberg, G. Quast, K. Rabbertz, D. Savoie, D. Schäfer, M. Schnepf, M. Schröder, I. Shvetsov, H.J. Simonis, R. Ulrich, M. Wassmer, M. Weber, C. Wöhrmann, R. Wolf, S. Wozniowski

Institute of Nuclear and Particle Physics (INPP), NCSR Demokritos, Aghia Paraskevi, Greece

G. Anagnostou, P. Asenov, G. Daskalakis, T. Geralis, A. Kyriakis, D. Loukas, G. Paspalaki, A. Stakia

National and Kapodistrian University of Athens, Athens, Greece

M. Diamantopoulou, G. Karathanasis, P. Kontaxakis, A. Manousakis-katsikakis, A. Panagiotou, I. Papavergou, N. Saoulidou, K. Theofilatos, K. Vellidis, E. Vourliotis

National Technical University of Athens, Athens, Greece

G. Bakas, K. Kousouris, I. Papakrivopoulos, G. Tsipolitis, A. Zacharopoulou

University of Ioánnina, Ioánnina, Greece

I. Evangelou, C. Foudas, P. Giannelis, P. Katsoulis, P. Kokkas, S. Mallios, K. Manitará, N. Manthos, I. Papadopoulos, J. Strogas, F.A. Triantis, D. Tsitsonis

MTA-ELTE Lendület CMS Particle and Nuclear Physics Group, Eötvös Loránd University, Budapest, Hungary

M. Bartók²¹, R. Chudasama, M. Csanad, P. Major, K. Mandal, A. Mehta, G. Pasztor, O. Surányi, G.I. Veres

Wigner Research Centre for Physics, Budapest, Hungary

G. Bencze, C. Hajdu, D. Horvath²², F. Sikler, V. Veszpremi, G. Vesztergombi[†]

Institute of Nuclear Research ATOMKI, Debrecen, Hungary

N. Beni, S. Czellar, J. Karancsi²¹, J. Molnar, Z. Szillasi

Institute of Physics, University of Debrecen, Debrecen, Hungary

P. Raics, D. Teyssier, Z.L. Trocsanyi, B. Ujvari

Eszterhazy Karoly University, Karoly Robert Campus, Gyongyos, Hungary

T. Csorgo, W.J. Metzger, F. Nemes, T. Novak

Indian Institute of Science (IISc), Bangalore, India

S. Choudhury, J.R. Komaragiri, P.C. Tiwari

National Institute of Science Education and Research, HBNI, Bhubaneswar, India

S. Bahinipati²⁴, C. Kar, G. Kole, P. Mal, V.K. Muraleedharan Nair Bindhu, A. Nayak²⁵, D.K. Sahoo²⁴, S.K. Swain

Panjab University, Chandigarh, India

S. Bansal, S.B. Beri, V. Bhatnagar, S. Chauhan, N. Dhingra²⁶, R. Gupta, A. Kaur, M. Kaur, S. Kaur, P. Kumari, M. Lohan, M. Meena, K. Sandeep, S. Sharma, J.B. Singh, A.K. Viridi

University of Delhi, Delhi, India

A. Bhardwaj, B.C. Choudhary, R.B. Garg, M. Gola, S. Keshri, Ashok Kumar, M. Naimuddin, P. Priyanka, K. Ranjan, Aashaq Shah, R. Sharma

Saha Institute of Nuclear Physics, HBNI, Kolkata, India

R. Bhardwaj²⁷, M. Bharti²⁷, R. Bhattacharya, S. Bhattacharya, U. Bhawandeep²⁷, D. Bhowmik, S. Dutta, S. Ghosh, B. Gomber²⁸, M. Maity²⁹, K. Mondal, S. Nandan, A. Purohit, P.K. Rout, G. Saha, S. Sarkar, M. Sharan, B. Singh²⁷, S. Thakur²⁷

Indian Institute of Technology Madras, Madras, India

P.K. Behera, S.C. Behera, P. Kalbhor, A. Muhammad, P.R. Pujahari, A. Sharma, A.K. Sikdar

Bhabha Atomic Research Centre, Mumbai, India

D. Dutta, V. Jha, D.K. Mishra, P.K. Netrakanti, L.M. Pant, P. Shukla

Tata Institute of Fundamental Research-A, Mumbai, India

T. Aziz, M.A. Bhat, S. Dugad, G.B. Mohanty, N. Sur, RavindraKumar Verma

Tata Institute of Fundamental Research-B, Mumbai, India

S. Banerjee, S. Bhattacharya, S. Chatterjee, P. Das, M. Guchait, S. Karmakar, S. Kumar, G. Majumder, K. Mazumdar, N. Sahoo, S. Sawant

Indian Institute of Science Education and Research (IISER), Pune, India

S. Dube, B. Kansal, A. Kapoor, K. Kothekar, S. Pandey, A. Rane, A. Rastogi, S. Sharma

Institute for Research in Fundamental Sciences (IPM), Tehran, Iran

S. Chenarani, S.M. Etesami, M. Khakzad, M. Mohammadi Najafabadi, M. Naseri, F. Rezaei Hosseinabadi

University College Dublin, Dublin, Ireland

M. Felcini, M. Grunewald

INFN Sezione di Bari ^a, Università di Bari ^b, Politecnico di Bari ^c, Bari, Italy

M. Abbrescia^{a,b}, R. Aly^{a,b,30}, C. Calabria^{a,b}, A. Colaleo^a, D. Creanza^{a,c}, L. Cristella^{a,b}, N. De Filippis^{a,c}, M. De Palma^{a,b}, A. Di Florio^{a,b}, W. Elmetenawee^{a,b}, L. Fiore^a, A. Gelmi^{a,b}, G. Iaselli^{a,c}, M. Ince^{a,b}, S. Lezki^{a,b}, G. Maggi^{a,c}, M. Maggi^a, J.A. Merlin^a, G. Miniello^{a,b}, S. My^{a,b},

S. Nuzzo^{a,b}, A. Pompili^{a,b}, G. Pugliese^{a,c}, R. Radogna^a, A. Ranieri^a, G. Selvaggi^{a,b}, L. Silvestris^a, F.M. Simone^{a,b}, R. Venditti^a, P. Verwilligen^a

INFN Sezione di Bologna ^a, Università di Bologna ^b, Bologna, Italy

G. Abbiendi^a, C. Battilana^{a,b}, D. Bonacorsi^{a,b}, L. Borgonovi^{a,b}, S. Braibant-Giacomelli^{a,b}, R. Campanini^{a,b}, P. Capiluppi^{a,b}, A. Castro^{a,b}, F.R. Cavallo^a, C. Ciocca^a, G. Codispoti^{a,b}, M. Cuffiani^{a,b}, G.M. Dallavalle^a, F. Fabbri^a, A. Fanfani^{a,b}, E. Fontanesi^{a,b}, P. Giacomelli^a, C. Grandi^a, L. Guiducci^{a,b}, F. Iemmi^{a,b}, S. Lo Meo^{a,31}, S. Marcellini^a, G. Masetti^a, F.L. Navarria^{a,b}, A. Perrotta^a, F. Primavera^{a,b}, A.M. Rossi^{a,b}, T. Rovelli^{a,b}, G.P. Siroli^{a,b}, N. Tosi^a

INFN Sezione di Catania ^a, Università di Catania ^b, Catania, Italy

S. Albergo^{a,b,32}, S. Costa^{a,b}, A. Di Mattia^a, R. Potenza^{a,b}, A. Tricomi^{a,b,32}, C. Tuve^{a,b}

INFN Sezione di Firenze ^a, Università di Firenze ^b, Firenze, Italy

G. Barbagli^a, A. Cassese^a, R. Ceccarelli^{a,b}, V. Ciulli^{a,b}, C. Civinini^a, R. D'Alessandro^{a,b}, F. Fiori^{a,c}, E. Focardi^{a,b}, G. Latino^{a,b}, P. Lenzi^{a,b}, M. Lizzo^{a,b}, M. Meschini^a, S. Paoletti^a, R. Seidita^{a,b}, G. Sguazzoni^a, L. Viliani^a

INFN Laboratori Nazionali di Frascati, Frascati, Italy

L. Benussi, S. Bianco, D. Piccolo

INFN Sezione di Genova ^a, Università di Genova ^b, Genova, Italy

M. Bozzo^{a,b}, F. Ferro^a, R. Mulargia^{a,b}, E. Robutti^a, S. Tosi^{a,b}

INFN Sezione di Milano-Bicocca ^a, Università di Milano-Bicocca ^b, Milano, Italy

A. Benaglia^a, A. Beschi^{a,b}, F. Brivio^{a,b}, V. Cirio^{a,b,17}, M.E. Dinardo^{a,b}, P. Dini^a, S. Gennai^a, A. Ghezzi^{a,b}, P. Govoni^{a,b}, L. Guzzi^{a,b}, M. Malberti^a, S. Malvezzi^a, D. Menasce^a, F. Monti^{a,b}, L. Moroni^a, M. Paganoni^{a,b}, D. Pedrini^a, S. Ragazzi^{a,b}, T. Tabarelli de Fatis^{a,b}, D. Valsecchi^{a,b,17}, D. Zuolo^{a,b}

INFN Sezione di Napoli ^a, Università di Napoli 'Federico II' ^b, Napoli, Italy, Università della Basilicata ^c, Potenza, Italy, Università G. Marconi ^d, Roma, Italy

S. Buontempo^a, N. Cavallo^{a,c}, A. De Iorio^{a,b}, A. Di Crescenzo^{a,b}, F. Fabozzi^{a,c}, F. Fienga^a, G. Galati^a, A.O.M. Iorio^{a,b}, L. Layer^{a,b}, L. Lista^{a,b}, S. Meola^{a,d,17}, P. Paolucci^{a,17}, B. Rossi^a, C. Sciacca^{a,b}, E. Voevodina^{a,b}

INFN Sezione di Padova ^a, Università di Padova ^b, Padova, Italy, Università di Trento ^c, Trento, Italy

P. Azzi^a, N. Bacchetta^a, D. Bisello^{a,b}, A. Boletti^{a,b}, A. Bragagnolo^{a,b}, R. Carlin^{a,b}, P. Checchia^a, P. De Castro Manzano^a, T. Dorigo^a, U. Dosselli^a, F. Gasparini^{a,b}, U. Gasparini^{a,b}, A. Gozzelino^a, S.Y. Hoh^{a,b}, M. Margoni^{a,b}, A.T. Meneguzzo^{a,b}, J. Pazzini^{a,b}, M. Presilla^b, P. Ronchese^{a,b}, R. Rossin^{a,b}, F. Simonetto^{a,b}, A. Tiko^a, M. Tosi^{a,b}, M. Zanetti^{a,b}, P. Zotto^{a,b}, A. Zucchetta^{a,b}, G. Zumerle^{a,b}

INFN Sezione di Pavia ^a, Università di Pavia ^b, Pavia, Italy

A. Braghieri^a, D. Fiorina^{a,b}, P. Montagna^{a,b}, S.P. Ratti^{a,b}, V. Re^a, M. Ressegotti^{a,b}, C. Riccardi^{a,b}, P. Salvini^a, I. Vai^a, P. Vitulo^{a,b}

INFN Sezione di Perugia ^a, Università di Perugia ^b, Perugia, Italy

M. Biasini^{a,b}, G.M. Bilei^a, D. Ciangottini^{a,b}, L. Fanò^{a,b}, P. Lariccia^{a,b}, R. Leonardi^{a,b}, E. Manoni^a, G. Mantovani^{a,b}, V. Mariani^{a,b}, M. Menichelli^a, A. Rossi^{a,b}, A. Santocchia^{a,b}, D. Spiga^a

INFN Sezione di Pisa ^a, Università di Pisa ^b, Scuola Normale Superiore di Pisa ^c, Pisa, Italy

K. Androsov^a, P. Azzurri^a, G. Bagliesi^a, V. Bertacchi^{a,c}, L. Bianchini^a, T. Boccali^a, R. Castaldi^a, M.A. Ciocci^{a,b}, R. Dell'Orso^a, S. Donato^a, L. Giannini^{a,c}, A. Giassi^a, M.T. Grippo^a,

F. Ligabue^{a,c}, E. Manca^{a,c}, G. Mandorli^{a,c}, A. Messineo^{a,b}, F. Palla^a, A. Rizzi^{a,b}, G. Rolandi^{a,c}, S. Roy Chowdhury^{a,c}, A. Scribano^a, P. Spagnolo^a, R. Tenchini^a, G. Tonelli^{a,b}, N. Turini^a, A. Venturi^a, P.G. Verdini^a

INFN Sezione di Roma ^a, Sapienza Università di Roma ^b, Rome, Italy

F. Cavallari^a, M. Cipriani^{a,b}, D. Del Re^{a,b}, E. Di Marco^a, M. Diemoz^a, E. Longo^{a,b}, P. Meridiani^a, G. Organtini^{a,b}, F. Pandolfi^a, R. Paramatti^{a,b}, C. Quaranta^{a,b}, S. Rahatlou^{a,b}, C. Rovelli^a, F. Santanastasio^{a,b}, L. Soffi^{a,b}, R. Tramontano^{a,b}

INFN Sezione di Torino ^a, Università di Torino ^b, Torino, Italy, Università del Piemonte Orientale ^c, Novara, Italy

N. Amapane^{a,b}, R. Arcidiacono^{a,c}, S. Argiro^{a,b}, M. Arneodo^{a,c}, N. Bartosik^a, R. Bellan^{a,b}, A. Bellora^{a,b}, C. Biino^a, A. Cappati^{a,b}, N. Cartiglia^a, S. Cometti^a, M. Costa^{a,b}, R. Covarelli^{a,b}, N. Demaria^a, J.R. González Fernández^a, B. Kiani^{a,b}, F. Legger^a, C. Mariotti^a, S. Maselli^a, E. Migliore^{a,b}, V. Monaco^{a,b}, E. Monteil^{a,b}, M. Monteno^a, M.M. Obertino^{a,b}, G. Ortona^a, L. Pacher^{a,b}, N. Pastrone^a, M. Pelliccioni^a, G.L. Pinna Angioni^{a,b}, A. Romero^{a,b}, M. Ruspa^{a,c}, R. Salvatico^{a,b}, V. Sola^a, A. Solano^{a,b}, D. Soldi^{a,b}, A. Staiano^a, D. Trocino^{a,b}

INFN Sezione di Trieste ^a, Università di Trieste ^b, Trieste, Italy

S. Belforte^a, V. Candelise^{a,b}, M. Casarsa^a, F. Cossutti^a, A. Da Rold^{a,b}, G. Della Ricca^{a,b}, F. Vazzoler^{a,b}, A. Zanetti^a

Kyungpook National University, Daegu, Korea

B. Kim, D.H. Kim, G.N. Kim, J. Lee, S.W. Lee, C.S. Moon, Y.D. Oh, S.I. Pak, S. Sekmen, D.C. Son, Y.C. Yang

Chonnam National University, Institute for Universe and Elementary Particles, Kwangju, Korea

H. Kim, D.H. Moon

Hanyang University, Seoul, Korea

B. Francois, T.J. Kim, J. Park

Korea University, Seoul, Korea

S. Cho, S. Choi, Y. Go, S. Ha, B. Hong, K. Lee, K.S. Lee, J. Lim, J. Park, S.K. Park, Y. Roh, J. Yoo

Kyung Hee University, Department of Physics

J. Goh

Sejong University, Seoul, Korea

H.S. Kim

Seoul National University, Seoul, Korea

J. Almond, J.H. Bhyun, J. Choi, S. Jeon, J. Kim, J.S. Kim, H. Lee, K. Lee, S. Lee, K. Nam, M. Oh, S.B. Oh, B.C. Radburn-Smith, U.K. Yang, H.D. Yoo, I. Yoon

University of Seoul, Seoul, Korea

D. Jeon, J.H. Kim, J.S.H. Lee, I.C. Park, I.J. Watson

Sungkyunkwan University, Suwon, Korea

Y. Choi, C. Hwang, Y. Jeong, J. Lee, Y. Lee, I. Yu

Riga Technical University, Riga, Latvia

V. Veckalns³³

Vilnius University, Vilnius, Lithuania

V. Dudenas, A. Juodagalvis, A. Rinkevicius, G. Tamulaitis, J. Vaitkus

National Centre for Particle Physics, Universiti Malaya, Kuala Lumpur, Malaysia

F. Mohamad Idris³⁴, W.A.T. Wan Abdullah, M.N. Yusli, Z. Zolkapli

Universidad de Sonora (UNISON), Hermosillo, Mexico

J.F. Benitez, A. Castaneda Hernandez, J.A. Murillo Quijada, L. Valencia Palomo

Centro de Investigacion y de Estudios Avanzados del IPN, Mexico City, Mexico

H. Castilla-Valdez, E. De La Cruz-Burelo, I. Heredia-De La Cruz³⁵, R. Lopez-Fernandez, A. Sanchez-Hernandez

Universidad Iberoamericana, Mexico City, Mexico

S. Carrillo Moreno, C. Oropeza Barrera, M. Ramirez-Garcia, F. Vazquez Valencia

Benemerita Universidad Autonoma de Puebla, Puebla, Mexico

J. Eysermans, I. Pedraza, H.A. Salazar Ibarquen, C. Uribe Estrada

Universidad Autónoma de San Luis Potosí, San Luis Potosí, Mexico

A. Morelos Pineda

University of Montenegro, Podgorica, Montenegro

J. Mijuskovic³, N. Raicevic

University of Auckland, Auckland, New Zealand

D. Krofcheck

University of Canterbury, Christchurch, New Zealand

S. Bheesette, P.H. Butler, P. Lujan

National Centre for Physics, Quaid-I-Azam University, Islamabad, Pakistan

A. Ahmad, M. Ahmad, M.I.M. Awan, Q. Hassan, H.R. Hoorani, W.A. Khan, M.A. Shah, M. Shoaib, M. Waqas

AGH University of Science and Technology Faculty of Computer Science, Electronics and Telecommunications, Krakow, Poland

V. Avati, L. Grzanka, M. Malawski

National Centre for Nuclear Research, Swierk, Poland

H. Bialkowska, M. Bluj, B. Boimska, M. Górski, M. Kazana, M. Szleper, P. Zalewski

Institute of Experimental Physics, Faculty of Physics, University of Warsaw, Warsaw, Poland

K. Bunkowski, A. Byszuk³⁶, K. Doroba, A. Kalinowski, M. Konecki, J. Krolikowski, M. Olszewski, M. Walczak

Laboratório de Instrumentação e Física Experimental de Partículas, Lisboa, Portugal

M. Araujo, P. Bargassa, D. Bastos, A. Di Francesco, P. Faccioli, B. Galinhas, M. Gallinaro, J. Hollar, N. Leonardo, T. Niknejad, J. Seixas, K. Shchelina, G. Strong, O. Toldaiev, J. Varela

Joint Institute for Nuclear Research, Dubna, Russia

V. Alexakhin, P. Bunin, Y. Ershov, I. Golutvin, N. Gorbounov, I. Gorbunov, A. Kamenev, V. Karjavine, A. Lanev, A. Malakhov, V. Matveev^{37,38}, P. Moiseenz, V. Palichik, V. Perelygin, M. Savina, S. Shmatov, N. Skatchkov, V. Smirnov, B.S. Yuldashev³⁹, A. Zarubin

Petersburg Nuclear Physics Institute, Gatchina (St. Petersburg), Russia

L. Chtchipounov, V. Golovtsov, Y. Ivanov, V. Kim⁴⁰, E. Kuznetsova⁴¹, P. Levchenko, V. Murzin, V. Oreshkin, I. Smirnov, D. Sosnov, V. Sulimov, L. Uvarov, A. Vorobyev

Institute for Nuclear Research, Moscow, Russia

Yu. Andreev, A. Dermenev, S. Gninenko, N. Golubev, A. Karneyeu, M. Kirsanov, N. Krasnikov, A. Pashenkov, D. Tlisov, A. Toropin

Institute for Theoretical and Experimental Physics named by A.I. Alikhanov of NRC 'Kurchatov Institute', Moscow, Russia

V. Epshteyn, V. Gavrilov, N. Lychkovskaya, A. Nikitenko⁴², V. Popov, I. Pozdnyakov, G. Safronov, A. Spiridonov, A. Stepenov, M. Toms, E. Vlasov, A. Zhokin

Moscow Institute of Physics and Technology, Moscow, Russia

T. Aushev

National Research Nuclear University 'Moscow Engineering Physics Institute' (MEPhI), Moscow, Russia

O. Bychkova, R. Chistov⁴³, M. Danilov⁴³, S. Polikarpov⁴³, E. Tarkovskii

P.N. Lebedev Physical Institute, Moscow, Russia

V. Andreev, M. Azarkin, I. Dremin, M. Kirakosyan, A. Terkulov

Skobeltsyn Institute of Nuclear Physics, Lomonosov Moscow State University, Moscow, Russia

A. Baskakov, A. Belyaev, E. Boos, V. Bunichev, M. Dubinin⁴⁴, L. Dudko, V. Klyukhin, N. Korneeva, I. Lokhtin, S. Obraztsov, M. Perfilov, V. Savrin, P. Volkov

Novosibirsk State University (NSU), Novosibirsk, Russia

A. Barnyakov⁴⁵, V. Blinov⁴⁵, T. Dimova⁴⁵, L. Kardapol'tsev⁴⁵, Y. Skovpen⁴⁵

Institute for High Energy Physics of National Research Centre 'Kurchatov Institute', Protvino, Russia

I. Azhgirey, I. Bayshev, S. Bitioukov, V. Kachanov, D. Konstantinov, P. Mandrik, V. Petrov, R. Ryutin, S. Slabospitskii, A. Sobol, S. Troshin, N. Tyurin, A. Uzunian, A. Volkov

National Research Tomsk Polytechnic University, Tomsk, Russia

A. Babaev, A. Iuzhakov, V. Okhotnikov

Tomsk State University, Tomsk, Russia

V. Borchsh, V. Ivanchenko, E. Tcherniaev

University of Belgrade: Faculty of Physics and VINCA Institute of Nuclear Sciences

P. Adzic⁴⁶, P. Cirkovic, M. Dordevic, P. Milenovic, J. Milosevic, M. Stojanovic

Centro de Investigaciones Energéticas Medioambientales y Tecnológicas (CIEMAT), Madrid, Spain

M. Aguilar-Benitez, J. Alcaraz Maestre, A. Álvarez Fernández, I. Bachiller, M. Barrio Luna, Cristina F. Bedoya, J.A. Brochero Cifuentes, C.A. Carrillo Montoya, M. Cepeda, M. Cerrada, N. Colino, B. De La Cruz, A. Delgado Peris, J.P. Fernández Ramos, J. Flix, M.C. Fouz, O. Gonzalez Lopez, S. Goy Lopez, J.M. Hernandez, M.I. Josa, D. Moran, Á. Navarro Tobar, A. Pérez-Calero Yzquierdo, J. Puerta Pelayo, I. Redondo, L. Romero, S. Sánchez Navas, M.S. Soares, A. Triossi, C. Willmott

Universidad Autónoma de Madrid, Madrid, Spain

C. Albajar, J.F. de Trocóniz, R. Reyes-Almanza

Universidad de Oviedo, Instituto Universitario de Ciencias y Tecnologías Espaciales de Asturias (ICTEA), Oviedo, Spain

B. Alvarez Gonzalez, J. Cuevas, C. Erice, J. Fernandez Menendez, S. Folgueras, I. Gonzalez Caballero, E. Palencia Cortezon, C. Ramón Álvarez, V. Rodríguez Bouza, S. Sanchez Cruz

Instituto de Física de Cantabria (IFCA), CSIC-Universidad de Cantabria, Santander, Spain

I.J. Cabrillo, A. Calderon, B. Chazin Quero, J. Duarte Campderros, M. Fernandez, P.J. Fernández Manteca, A. García Alonso, G. Gomez, C. Martinez Rivero, P. Martinez Ruiz del Arbol, F. Matorras, J. Piedra Gomez, C. Prieels, F. Ricci-Tam, T. Rodrigo, A. Ruiz-Jimeno, L. Russo⁴⁷, L. Scodellaro, I. Vila, J.M. Vizán Garcia

University of Colombo, Colombo, Sri Lanka

D.U.J. Sonnadara

University of Ruhuna, Department of Physics, Matara, Sri Lanka

W.G.D. Dharmaratna, N. Wickramage

CERN, European Organization for Nuclear Research, Geneva, Switzerland

T.K. Aarrestad, D. Abbaneo, B. Akgun, E. Auffray, G. Auzinger, J. Baechler, P. Baillon, A.H. Ball, D. Barney, J. Bendavid, M. Bianco, A. Bocci, P. Bortignon, E. Bossini, E. Brondolin, T. Camporesi, A. Caratelli, G. Cerminara, E. Chapon, G. Cucciati, D. d'Enterria, A. Dabrowski, N. Daci, V. Daponte, A. David, O. Davignon, A. De Roeck, M. Deile, R. Di Maria, M. Dobson, M. Dünser, N. Dupont, A. Elliott-Peisert, N. Emriskova, F. Fallavollita⁴⁸, D. Fasanella, S. Fiorendi, G. Franzoni, J. Fulcher, W. Funk, S. Giani, D. Gigi, K. Gill, F. Glege, L. Gouskos, M. Gruchala, M. Guilbaud, D. Gulhan, J. Hegeman, C. Heidegger, Y. Iiyama, V. Innocente, T. James, P. Janot, O. Karacheban²⁰, J. Kaspar, J. Kieseler, M. Krammer¹, N. Kratochwil, C. Lange, P. Lecoq, K. Long, C. Lourenço, L. Malgeri, M. Mannelli, A. Massironi, F. Meijers, S. Mersi, E. Meschi, F. Moortgat, M. Mulders, J. Ngadiuba, J. Niedziela, S. Nourbakhsh, S. Orfanelli, L. Orsini, F. Pantaleo¹⁷, L. Pape, E. Perez, M. Peruzzi, A. Petrilli, G. Petrucciani, A. Pfeiffer, M. Pierini, F.M. Pitters, D. Rabadý, A. Racz, M. Rieger, M. Rovere, H. Sakulin, J. Salfeld-Nebgen, S. Scarfi, C. Schäfer, C. Schwick, M. Selvaggi, A. Sharma, P. Silva, W. Snoeys, P. Sphicas⁴⁹, J. Steggemann, S. Summers, V.R. Tavolaro, D. Treille, A. Tsiros, G.P. Van Onsem, A. Vartak, M. Verzetti, K.A. Wozniak, W.D. Zeuner

Paul Scherrer Institut, Villigen, Switzerland

L. Caminada⁵⁰, K. Deiters, W. Erdmann, R. Horisberger, Q. Ingram, H.C. Kaestli, D. Kotlinski, U. Langenegger, T. Rohe

ETH Zurich - Institute for Particle Physics and Astrophysics (IPA), Zurich, Switzerland

M. Backhaus, P. Berger, A. Calandri, N. Chernyavskaya, G. Dissertori, M. Dittmar, M. Donegà, C. Dorfer, T.A. Gómez Espinosa, C. Grab, D. Hits, W. Luster, R.A. Manzoni, M.T. Meinhard, F. Micheli, P. Musella, F. Nessi-Tedaldi, F. Pauss, V. Perovic, G. Perrin, L. Perrozzi, S. Pigazzini, M.G. Ratti, M. Reichmann, C. Reissel, T. Reitenspiess, B. Ristic, D. Ruini, D.A. Sanz Becerra, M. Schönenberger, L. Shchutska, M.L. Vesterbacka Olsson, R. Wallny, D.H. Zhu

Universität Zürich, Zurich, Switzerland

C. Amsler⁵¹, C. Botta, D. Brzhechko, M.F. Canelli, A. De Cosa, R. Del Burgo, B. Kilminster, S. Leontsinis, V.M. Mikuni, I. Neutelings, G. Rauco, P. Robmann, K. Schweiger, Y. Takahashi, S. Wertz

National Central University, Chung-Li, Taiwan

C.M. Kuo, W. Lin, A. Roy, T. Sarkar²⁹, S.S. Yu

National Taiwan University (NTU), Taipei, Taiwan

P. Chang, Y. Chao, K.F. Chen, P.H. Chen, W.-S. Hou, Y.y. Li, R.-S. Lu, E. Paganis, A. Psallidas, A. Steen

Chulalongkorn University, Faculty of Science, Department of Physics, Bangkok, Thailand

B. Asavapibhop, C. Asawatangtrakuldee, N. Srimanobhas, N. Suwonjandee

Çukurova University, Physics Department, Science and Art Faculty, Adana, Turkey

A. Bat, F. Boran, A. Celik⁵², S. Damarseckin⁵³, Z.S. Demiroglu, F. Dolek, C. Dozen⁵⁴, I. Dumanoglu⁵⁵, G. Gokbulut, EmineGurpinar Guler⁵⁶, Y. Guler, I. Hos⁵⁷, C. Isik, E.E. Kangal⁵⁸, O. Kara, A. Kayis Topaksu, U. Kiminsu, G. Onengut, K. Ozdemir⁵⁹, A.E. Simsek, U.G. Tok, S. Turkcapar, I.S. Zorbakir, C. Zorbilmez

Middle East Technical University, Physics Department, Ankara, Turkey

B. Isildak⁶⁰, G. Karapinar⁶¹, M. Yalvac⁶²

Bogazici University, Istanbul, Turkey

I.O. Atakisi, E. Gülmez, M. Kaya⁶³, O. Kaya⁶⁴, Ö. Özçelik, S. Tekten⁶⁵, E.A. Yetkin⁶⁶

Istanbul Technical University, Istanbul, Turkey

A. Cakir, K. Cankocak⁵⁵, Y. Komurcu, S. Sen⁶⁷

Istanbul University, Istanbul, Turkey

S. Cerci⁶⁸, B. Kaynak, S. Ozkorucuklu, D. Sunar Cerci⁶⁸

Institute for Scintillation Materials of National Academy of Science of Ukraine, Kharkov, Ukraine

B. Grynyov

National Scientific Center, Kharkov Institute of Physics and Technology, Kharkov, Ukraine

L. Levchuk

University of Bristol, Bristol, United Kingdom

E. Bhal, S. Bologna, J.J. Brooke, D. Burns⁶⁹, E. Clement, D. Cussans, H. Flacher, J. Goldstein, G.P. Heath, H.F. Heath, L. Kreczko, B. Krikler, S. Paramesvaran, T. Sakuma, S. Seif El Nasr-Storey, V.J. Smith, J. Taylor, A. Titterton

Rutherford Appleton Laboratory, Didcot, United Kingdom

K.W. Bell, A. Belyaev⁷⁰, C. Brew, R.M. Brown, D.J.A. Cockerill, J.A. Coughlan, K. Harder, S. Harper, J. Linacre, K. Manolopoulos, D.M. Newbold, E. Olaiya, D. Petyt, T. Reis, T. Schuh, C.H. Shepherd-Themistocleous, A. Thea, I.R. Tomalin, T. Williams

Imperial College, London, United Kingdom

R. Bainbridge, P. Bloch, S. Bonomally, J. Borg, S. Breeze, O. Buchmuller, A. Bundock, GurpreetSingh CHAHAL⁷¹, D. Colling, P. Dauncey, G. Davies, M. Della Negra, P. Everaerts, G. Hall, G. Iles, M. Komm, J. Langford, L. Lyons, A.-M. Magnan, S. Malik, A. Martelli, V. Milosevic, A. Morton, J. Nash⁷², V. Palladino, M. Pesaresi, D.M. Raymond, A. Richards, A. Rose, E. Scott, C. Seez, A. Shtipliyski, M. Stoye, T. Strebler, A. Tapper, K. Uchida, T. Virdee¹⁷, N. Wardle, S.N. Webb, D. Winterbottom, A.G. Zecchinelli, S.C. Zenz

Brunel University, Uxbridge, United Kingdom

J.E. Cole, P.R. Hobson, A. Khan, P. Kyberd, C.K. Mackay, I.D. Reid, L. Teodorescu, S. Zahid

Baylor University, Waco, USA

A. Brinkerhoff, K. Call, B. Caraway, J. Dittmann, K. Hatakeyama, C. Madrid, B. McMaster, N. Pastika, C. Smith

Catholic University of America, Washington, DC, USA

R. Bartek, A. Dominguez, R. Uniyal, A.M. Vargas Hernandez

The University of Alabama, Tuscaloosa, USA

A. Buccilli, S.I. Cooper, S.V. Gleyzer, C. Henderson, P. Rumerio, C. West

Boston University, Boston, USA

A. Albert, D. Arcaro, Z. Demiragli, D. Gastler, C. Richardson, J. Rohlf, D. Sperka, D. Spitzbart, I. Suarez, L. Sulak, D. Zou

Brown University, Providence, USA

G. Benelli, B. Burkle, X. Coubez¹⁸, D. Cutts, Y.t. Duh, M. Hadley, U. Heintz, J.M. Hogan⁷³, K.H.M. Kwok, E. Laird, G. Landsberg, K.T. Lau, J. Lee, M. Narain, S. Sagir⁷⁴, R. Syarif, E. Usai, W.Y. Wong, D. Yu, W. Zhang

University of California, Davis, Davis, USA

R. Band, C. Brainerd, R. Breedon, M. Calderon De La Barca Sanchez, M. Chertok, J. Conway, R. Conway, P.T. Cox, R. Erbacher, C. Flores, G. Funk, F. Jensen, W. Ko[†], O. Kukral, R. Lander, M. Mulhearn, D. Pellett, J. Pilot, M. Shi, D. Taylor, K. Tos, M. Tripathi, Z. Wang, F. Zhang

University of California, Los Angeles, USA

M. Bachtis, C. Bravo, R. Cousins, A. Dasgupta, A. Florent, J. Hauser, M. Ignatenko, N. Mccoll, W.A. Nash, S. Regnard, D. Saltzberg, C. Schnaible, B. Stone, V. Valuev

University of California, Riverside, Riverside, USA

K. Burt, Y. Chen, R. Clare, J.W. Gary, S.M.A. Ghiasi Shirazi, G. Hanson, G. Karapostoli, O.R. Long, N. Manganelli, M. Olmedo Negrete, M.I. Paneva, W. Si, S. Wimpenny, B.R. Yates, Y. Zhang

University of California, San Diego, La Jolla, USA

J.G. Branson, P. Chang, S. Cittolin, S. Cooperstein, N. Deelen, M. Derdzinski, J. Duarte, R. Gerosa, D. Gilbert, B. Hashemi, D. Klein, V. Krutelyov, J. Letts, M. Masciovecchio, S. May, S. Padhi, M. Pieri, V. Sharma, M. Tadel, F. Würthwein, A. Yagil, G. Zevi Della Porta

University of California, Santa Barbara - Department of Physics, Santa Barbara, USA

N. Amin, R. Bhandari, C. Campagnari, M. Citron, V. Dutta, J. Incandela, B. Marsh, H. Mei, A. Ovcharova, H. Qu, J. Richman, U. Sarica, D. Stuart, S. Wang

California Institute of Technology, Pasadena, USA

D. Anderson, A. Bornheim, O. Cerri, I. Dutta, J.M. Lawhorn, N. Lu, J. Mao, H.B. Newman, T.Q. Nguyen, J. Pata, M. Spiropulu, J.R. Vlimant, S. Xie, Z. Zhang, R.Y. Zhu

Carnegie Mellon University, Pittsburgh, USA

J. Alison, M.B. Andrews, T. Ferguson, T. Mudholkar, M. Paulini, M. Sun, I. Vorobiev, M. Weinberg

University of Colorado Boulder, Boulder, USA

J.P. Cumalat, W.T. Ford, E. MacDonald, T. Mulholland, R. Patel, A. Perloff, K. Stenson, K.A. Ulmer, S.R. Wagner

Cornell University, Ithaca, USA

J. Alexander, Y. Cheng, J. Chu, A. Datta, A. Frankenthal, K. Mcdermott, J.R. Patterson, D. Quach, A. Ryd, S.M. Tan, Z. Tao, J. Thom, P. Wittich, M. Zientek

Fermi National Accelerator Laboratory, Batavia, USA

S. Abdullin, M. Albrow, M. Alyari, G. Apollinari, A. Apresyan, A. Apyan, S. Banerjee,

L.A.T. Bauerdick, A. Beretvas, D. Berry, J. Berryhill, P.C. Bhat, K. Burkett, J.N. Butler, A. Canepa, G.B. Cerati, H.W.K. Cheung, F. Chlebana, M. Cremonesi, V.D. Elvira, J. Freeman, Z. Gece, E. Gottschalk, L. Gray, D. Green, S. Grünendahl, O. Gutsche, J. Hanlon, R.M. Harris, S. Hasegawa, R. Heller, J. Hirschauer, B. Jayatilaka, S. Jindariani, M. Johnson, U. Joshi, T. Klijnsma, B. Klima, M.J. Kortelainen, B. Kreis, S. Lammel, J. Lewis, D. Lincoln, R. Lipton, M. Liu, T. Liu, J. Lykken, K. Maeshima, J.M. Marraffino, D. Mason, P. McBride, P. Merkel, S. Mrenna, S. Nahn, V. O'Dell, V. Papadimitriou, K. Pedro, C. Pena⁴⁴, F. Ravera, A. Reinsvold Hall, L. Ristori, B. Schneider, E. Sexton-Kennedy, N. Smith, A. Soha, W.J. Spalding, L. Spiegel, S. Stoynev, J. Strait, L. Taylor, S. Tkaczyk, N.V. Tran, L. Uplegger, E.W. Vaandering, R. Vidal, M. Wang, H.A. Weber, A. Woodard

University of Florida, Gainesville, USA

D. Acosta, P. Avery, D. Bourilkov, L. Cadamuro, V. Cherepanov, F. Errico, R.D. Field, D. Guerrero, B.M. Joshi, M. Kim, J. Konigsberg, A. Korytov, K.H. Lo, K. Matchev, N. Menendez, G. Mitselmakher, D. Rosenzweig, K. Shi, J. Wang, S. Wang, X. Zuo

Florida International University, Miami, USA

Y.R. Joshi

Florida State University, Tallahassee, USA

T. Adams, A. Askew, S. Hagopian, V. Hagopian, K.F. Johnson, R. Khurana, T. Kolberg, G. Martinez, T. Perry, H. Prosper, C. Schiber, R. Yohay, J. Zhang

Florida Institute of Technology, Melbourne, USA

M.M. Baarmand, M. Hohlmann, D. Noonan, M. Rahmani, M. Saunders, F. Yumiceva

University of Illinois at Chicago (UIC), Chicago, USA

M.R. Adams, L. Apanasevich, R.R. Betts, R. Cavanaugh, X. Chen, S. Dittmer, O. Evdokimov, C.E. Gerber, D.A. Hangal, D.J. Hofman, V. Kumar, C. Mills, G. Oh, T. Roy, M.B. Tonjes, N. Varelas, J. Viinikainen, H. Wang, X. Wang, Z. Wu

The University of Iowa, Iowa City, USA

M. Alhusseini, B. Bilki⁵⁶, K. Dilsiz⁷⁵, S. Durgut, R.P. Gandrajula, M. Haytmyradov, V. Khristenko, O.K. Köseyan, J.-P. Merlo, A. Mestvirishvili⁷⁶, A. Moeller, J. Nachtman, H. Ogul⁷⁷, Y. Onel, F. Ozok⁷⁸, A. Penzo, C. Snyder, E. Tiras, J. Wetzel, K. Yi⁷⁹

Johns Hopkins University, Baltimore, USA

B. Blumenfeld, A. Cocoros, N. Eminizer, A.V. Gritsan, W.T. Hung, S. Kyriacou, P. Maksimovic, C. Mantilla, J. Roskes, M. Swartz, T.Á. Vámi

The University of Kansas, Lawrence, USA

C. Baldenegro Barrera, P. Baringer, A. Bean, S. Boren, A. Bylinkin, T. Isidori, S. Khalil, J. King, G. Krintiras, A. Kropivnitskaya, C. Lindsey, D. Majumder, W. Mcbrayer, N. Minafra, M. Murray, C. Rogan, C. Royon, S. Sanders, E. Schmitz, J.D. Tapia Takaki, Q. Wang, J. Williams, G. Wilson

Kansas State University, Manhattan, USA

S. Duric, A. Ivanov, K. Kaadze, D. Kim, Y. Maravin, D.R. Mendis, T. Mitchell, A. Modak, A. Mohammadi

Lawrence Livermore National Laboratory, Livermore, USA

F. Rebassoo, D. Wright

University of Maryland, College Park, USA

A. Baden, O. Baron, A. Belloni, S.C. Eno, Y. Feng, N.J. Hadley, S. Jabeen, G.Y. Jeng, R.G. Kellogg, A.C. Mignerey, S. Nabili, M. Seidel, A. Skuja, S.C. Tonwar, L. Wang, K. Wong

Massachusetts Institute of Technology, Cambridge, USA

D. Abercrombie, B. Allen, R. Bi, S. Brandt, W. Busza, I.A. Cali, M. D'Alfonso, G. Gomez Ceballos, M. Goncharov, P. Harris, D. Hsu, M. Hu, M. Klute, D. Kovalskyi, Y.-J. Lee, P.D. Luckey, B. Maier, A.C. Marini, C. McGinn, C. Mironov, S. Narayanan, X. Niu, C. Paus, D. Rankin, C. Roland, G. Roland, Z. Shi, G.S.F. Stephans, K. Sumorok, K. Tatar, D. Velicanu, J. Wang, T.W. Wang, B. Wyslouch

University of Minnesota, Minneapolis, USA

R.M. Chatterjee, A. Evans, S. Guts[†], P. Hansen, J. Hiltbrand, Sh. Jain, Y. Kubota, Z. Lesko, J. Mans, M. Revering, R. Rusack, R. Saradhy, N. Schroeder, N. Strobbe, M.A. Wadud

University of Mississippi, Oxford, USA

J.G. Acosta, S. Oliveros

University of Nebraska-Lincoln, Lincoln, USA

K. Bloom, S. Chauhan, D.R. Claes, C. Fangmeier, L. Finco, F. Golf, R. Kamalieddin, I. Kravchenko, J.E. Siado, G.R. Snow[†], B. Stieger, W. Tabb

State University of New York at Buffalo, Buffalo, USA

G. Agarwal, C. Harrington, I. Iashvili, A. Kharchilava, C. McLean, D. Nguyen, A. Parker, J. Pekkanen, S. Rappoccio, B. Roozbahani

Northeastern University, Boston, USA

G. Alverson, E. Barberis, C. Freer, Y. Haddad, A. Hortiangtham, G. Madigan, B. Marzocchi, D.M. Morse, V. Nguyen, T. Orimoto, L. Skinnari, A. Tishelman-Charny, T. Wamorkar, B. Wang, A. Wisecarver, D. Wood

Northwestern University, Evanston, USA

S. Bhattacharya, J. Bueghly, G. Fedi, A. Gilbert, T. Gunter, K.A. Hahn, N. Odell, M.H. Schmitt, K. Sung, M. Velasco

University of Notre Dame, Notre Dame, USA

R. Bucci, N. Dev, R. Goldouzian, M. Hildreth, K. Hurtado Anampa, C. Jessop, D.J. Karmgard, K. Lannon, W. Li, N. Loukas, N. Marinelli, I. Mcalister, F. Meng, Y. Musienko³⁷, R. Ruchti, P. Siddireddy, G. Smith, S. Taroni, M. Wayne, A. Wightman, M. Wolf

The Ohio State University, Columbus, USA

J. Alimena, B. Bylsma, B. Cardwell, L.S. Durkin, B. Francis, C. Hill, W. Ji, A. Lefeld, T.Y. Ling, B.L. Winer

Princeton University, Princeton, USA

G. Dezoort, P. Elmer, J. Hardenbrook, N. Haubrich, S. Higginbotham, A. Kalogeropoulos, S. Kwan, D. Lange, M.T. Lucchini, J. Luo, D. Marlow, K. Mei, I. Ojalvo, J. Olsen, C. Palmer, P. Piroué, D. Stickland, C. Tully

University of Puerto Rico, Mayaguez, USA

S. Malik, S. Norberg

Purdue University, West Lafayette, USA

A. Barker, V.E. Barnes, R. Chawla, S. Das, L. Gutay, M. Jones, A.W. Jung, B. Mahakud, D.H. Miller, G. Negro, N. Neumeister, C.C. Peng, S. Piperov, H. Qiu, J.F. Schulte, N. Trevisani, F. Wang, R. Xiao, W. Xie

Purdue University Northwest, Hammond, USA

T. Cheng, J. Dolen, N. Parashar

Rice University, Houston, USA

A. Baty, U. Behrens, S. Dildick, K.M. Ecklund, S. Freed, F.J.M. Geurts, M. Kilpatrick, Arun Kumar, W. Li, B.P. Padley, R. Redjimi, J. Roberts, J. Rorie, W. Shi, A.G. Stahl Leitton, Z. Tu, A. Zhang

University of Rochester, Rochester, USA

A. Bodek, P. de Barbaro, R. Demina, J.L. Dulemba, C. Fallon, T. Ferbel, M. Galanti, A. Garcia-Bellido, O. Hindrichs, A. Khukhunaishvili, E. Ranken, R. Taus

Rutgers, The State University of New Jersey, Piscataway, USA

B. Chiarito, J.P. Chou, A. Gandrakota, Y. Gershtein, E. Halkiadakis, A. Hart, M. Heindl, E. Hughes, S. Kaplan, I. Laflotte, A. Lath, R. Montalvo, K. Nash, M. Osherson, S. Salur, S. Schnetzer, S. Somalwar, R. Stone, S. Thomas

University of Tennessee, Knoxville, USA

H. Acharya, A.G. Delannoy, S. Spanier

Texas A&M University, College Station, USA

O. Bouhali⁸⁰, M. Dalchenko, A. Delgado, R. Eusebi, J. Gilmore, T. Huang, T. Kamon⁸¹, H. Kim, S. Luo, S. Malhotra, D. Marley, R. Mueller, D. Overton, L. Perniè, D. Rathjens, A. Safonov

Texas Tech University, Lubbock, USA

N. Akchurin, J. Damgov, F. De Guio, V. Hegde, S. Kunori, K. Lamichhane, S.W. Lee, T. Mengke, S. Muthumuni, T. Peltola, S. Undleeb, I. Volobouev, Z. Wang, A. Whitbeck

Vanderbilt University, Nashville, USA

S. Greene, A. Gurrola, R. Janjam, W. Johns, C. Maguire, A. Melo, H. Ni, K. Padeken, F. Romeo, P. Sheldon, S. Tuo, J. Velkovska, M. Verweij

University of Virginia, Charlottesville, USA

M.W. Arenton, P. Barria, B. Cox, G. Cummings, J. Hakala, R. Hirosky, M. Joyce, A. Ledovskoy, C. Neu, B. Tannenwald, Y. Wang, E. Wolfe, F. Xia

Wayne State University, Detroit, USA

R. Harr, P.E. Karchin, N. Poudyal, J. Sturdy, P. Thapa

University of Wisconsin - Madison, Madison, WI, USA

K. Black, T. Bose, J. Buchanan, C. Caillol, D. Carlsmith, S. Dasu, I. De Bruyn, L. Dodd, C. Galloni, H. He, M. Herndon, A. Hervé, U. Hussain, A. Lanaro, A. Loeliger, R. Loveless, J. Madhusudanan Sreekala, A. Mallampalli, D. Pinna, T. Ruggles, A. Savin, V. Sharma, W.H. Smith, D. Teague, S. Trembath-reichert

†: Deceased

1: Also at Vienna University of Technology, Vienna, Austria

2: Also at Université Libre de Bruxelles, Bruxelles, Belgium

3: Also at IRFU, CEA, Université Paris-Saclay, Gif-sur-Yvette, France

4: Also at Universidade Estadual de Campinas, Campinas, Brazil

5: Also at Federal University of Rio Grande do Sul, Porto Alegre, Brazil

6: Also at UFMS, Nova Andradina, Brazil

7: Also at Universidade Federal de Pelotas, Pelotas, Brazil

8: Also at University of Chinese Academy of Sciences, Beijing, China

9: Also at Institute for Theoretical and Experimental Physics named by A.I. Alikhanov of NRC 'Kurchatov Institute', Moscow, Russia

10: Also at Joint Institute for Nuclear Research, Dubna, Russia

- 11: Also at Helwan University, Cairo, Egypt
- 12: Now at Zewail City of Science and Technology, Zewail, Egypt
- 13: Also at Purdue University, West Lafayette, USA
- 14: Also at Université de Haute Alsace, Mulhouse, France
- 15: Also at Tbilisi State University, Tbilisi, Georgia
- 16: Also at Erzincan Binali Yildirim University, Erzincan, Turkey
- 17: Also at CERN, European Organization for Nuclear Research, Geneva, Switzerland
- 18: Also at RWTH Aachen University, III. Physikalisches Institut A, Aachen, Germany
- 19: Also at University of Hamburg, Hamburg, Germany
- 20: Also at Brandenburg University of Technology, Cottbus, Germany
- 21: Also at Institute of Physics, University of Debrecen, Debrecen, Hungary, Debrecen, Hungary
- 22: Also at Institute of Nuclear Research ATOMKI, Debrecen, Hungary
- 23: Also at MTA-ELTE Lendület CMS Particle and Nuclear Physics Group, Eötvös Loránd University, Budapest, Hungary, Budapest, Hungary
- 24: Also at IIT Bhubaneswar, Bhubaneswar, India, Bhubaneswar, India
- 25: Also at Institute of Physics, Bhubaneswar, India
- 26: Also at G.H.G. Khalsa College, Punjab, India
- 27: Also at Shoolini University, Solan, India
- 28: Also at University of Hyderabad, Hyderabad, India
- 29: Also at University of Visva-Bharati, Santiniketan, India
- 30: Now at INFN Sezione di Bari ^a, Università di Bari ^b, Politecnico di Bari ^c, Bari, Italy
- 31: Also at Italian National Agency for New Technologies, Energy and Sustainable Economic Development, Bologna, Italy
- 32: Also at Centro Siciliano di Fisica Nucleare e di Struttura Della Materia, Catania, Italy
- 33: Also at Riga Technical University, Riga, Latvia, Riga, Latvia
- 34: Also at Malaysian Nuclear Agency, MOSTI, Kajang, Malaysia
- 35: Also at Consejo Nacional de Ciencia y Tecnología, Mexico City, Mexico
- 36: Also at Warsaw University of Technology, Institute of Electronic Systems, Warsaw, Poland
- 37: Also at Institute for Nuclear Research, Moscow, Russia
- 38: Now at National Research Nuclear University 'Moscow Engineering Physics Institute' (MEPhI), Moscow, Russia
- 39: Also at Institute of Nuclear Physics of the Uzbekistan Academy of Sciences, Tashkent, Uzbekistan
- 40: Also at St. Petersburg State Polytechnical University, St. Petersburg, Russia
- 41: Also at University of Florida, Gainesville, USA
- 42: Also at Imperial College, London, United Kingdom
- 43: Also at P.N. Lebedev Physical Institute, Moscow, Russia
- 44: Also at California Institute of Technology, Pasadena, USA
- 45: Also at Budker Institute of Nuclear Physics, Novosibirsk, Russia
- 46: Also at Faculty of Physics, University of Belgrade, Belgrade, Serbia
- 47: Also at Università degli Studi di Siena, Siena, Italy
- 48: Also at INFN Sezione di Pavia ^a, Università di Pavia ^b, Pavia, Italy, Pavia, Italy
- 49: Also at National and Kapodistrian University of Athens, Athens, Greece
- 50: Also at Universität Zürich, Zurich, Switzerland
- 51: Also at Stefan Meyer Institute for Subatomic Physics, Vienna, Austria, Vienna, Austria
- 52: Also at Burdur Mehmet Akif Ersoy University, BURDUR, Turkey
- 53: Also at Şırnak University, Sirnak, Turkey
- 54: Also at Department of Physics, Tsinghua University, Beijing, China, Beijing, China

-
- 55: Also at Near East University, Research Center of Experimental Health Science, Nicosia, Turkey
- 56: Also at Beykent University, Istanbul, Turkey, Istanbul, Turkey
- 57: Also at Istanbul Aydin University, Application and Research Center for Advanced Studies (App. & Res. Cent. for Advanced Studies), Istanbul, Turkey
- 58: Also at Mersin University, Mersin, Turkey
- 59: Also at Piri Reis University, Istanbul, Turkey
- 60: Also at Ozyegin University, Istanbul, Turkey
- 61: Also at Izmir Institute of Technology, Izmir, Turkey
- 62: Also at Bozok Universitetesi Rektörlüğü, Yozgat, Turkey
- 63: Also at Marmara University, Istanbul, Turkey
- 64: Also at Milli Savunma University, Istanbul, Turkey
- 65: Also at Kafkas University, Kars, Turkey
- 66: Also at Istanbul Bilgi University, Istanbul, Turkey
- 67: Also at Hacettepe University, Ankara, Turkey
- 68: Also at Adiyaman University, Adiyaman, Turkey
- 69: Also at Vrije Universiteit Brussel, Brussel, Belgium
- 70: Also at School of Physics and Astronomy, University of Southampton, Southampton, United Kingdom
- 71: Also at IPPP Durham University, Durham, United Kingdom
- 72: Also at Monash University, Faculty of Science, Clayton, Australia
- 73: Also at Bethel University, St. Paul, Minneapolis, USA, St. Paul, USA
- 74: Also at Karamanoğlu Mehmetbey University, Karaman, Turkey
- 75: Also at Bingol University, Bingol, Turkey
- 76: Also at Georgian Technical University, Tbilisi, Georgia
- 77: Also at Sinop University, Sinop, Turkey
- 78: Also at Mimar Sinan University, Istanbul, Istanbul, Turkey
- 79: Also at Nanjing Normal University Department of Physics, Nanjing, China
- 80: Also at Texas A&M University at Qatar, Doha, Qatar
- 81: Also at Kyungpook National University, Daegu, Korea, Daegu, Korea